

Rnf111 has a pivotal role in regulating development of definitive hematopoietic stem and progenitor cells through the Smad2/3-Gcsfr/NO axis in zebrafish

by Xiaohui Liu, Jinghan Sha, Luxiang Wang, Zixuan Wang, Zhou Fang, Xiao Han, Shuiyi Tan, Yi Chen, Hao Yuan, Hugues de The, Jun Zhou, and Jun Zhu

Received: March 11, 2024.

Accepted: September 23, 2024.

Citation: Xiaohui Liu, Jinghan Sha, Luxiang Wang, Zixuan Wang, Zhou Fang, Xiao Han, Shuiyi Tan, Yi Chen, Hao Yuan, Hugues de The, Jun Zhou, and Jun Zhu. Rnf111 has a pivotal role in regulating development of definitive hematopoietic stem and progenitor cells through the Smad2/3-Gcsfr/NO axis in zebrafish.

Haematologica. 2024 Oct 3. doi: 10.3324/haematol.2024.285438 [Epub ahead of print]

Publisher's Disclaimer.

E-publishing ahead of print is increasingly important for the rapid dissemination of science. Haematologica is, therefore, E-publishing PDF files of an early version of manuscripts that have completed a regular peer review and have been accepted for publication.

E-publishing of this PDF file has been approved by the authors.

After having E-published Ahead of Print, manuscripts will then undergo technical and English editing, typesetting, proof correction and be presented for the authors' final approval; the final version of the manuscript will then appear in a regular issue of the journal.

All legal disclaimers that apply to the journal also pertain to this production process.

Rnf111 has a pivotal role in regulating development of definitive hematopoietic stem and progenitor cells through the Smad2/3-Gcsfr/NO axis in zebrafish

*Xiaohui Liu^{1,2}, *Jinghan Sha^{1,2}, Luxiang Wang¹, Zixuan Wang¹, Zhou Fang^{1,2}, Xiao Han¹, Shuiyi Tan^{1,2}, Yi Chen¹, Hao Yuan^{1,2}, Hugues de The^{2,3}, Jun Zhou^{1,2}, Jun Zhu^{2,3}

¹ Shanghai Institute of Hematology, State Key Laboratory of Medical Genomics, National Research Center for Translational Medicine at Shanghai, Ruijin Hospital, Shanghai Jiao Tong University School of Medicine, Shanghai 200025, China

² CNRS IRP (International research Project), Cancer, Aging and Hematology, Sino-French Research Center for Life Sciences and Genomics, Ruijin Hospital, Shanghai Jiao Tong University School of Medicine, Shanghai 200025, China

³ Université de Paris 7/INSERM/CNRS UMR 944/7212, Equipe Labellisée Ligue Nationale Contre le Cancer, Hôpital St. Louis, Paris 75010, France

Authors' contributions. XL and JS contributed equally as co-first authors. X.L. and J.S. performed the experiments and analyzed the data. L.W., Z.W., Z.F., X.H., S.T. and Y.C. assisted with the experiments. H.Y., H.d.T. and J.Z. provided suggestions on experimental design and data presentation. X.L. and J.Z. designed the research plan and wrote the paper. All authors read and approved the final manuscript. The authors declare no conflicts of interest.

Running head. Rnf111 maintains HSPCs *via* Smads-Gcsfr/NO axis

Corresponding author. Xiaohui Liu (liuxiaohuiuestc@126.com), Jun Zhu (jun.zhu@paris7.jussieu.fr or zhuj1966@yahoo.com).

Data-sharing statement. The data involved in this study are available upon reasonable request from the corresponding author.

Word count. The abstract contains 150 words and the main text contains 3908 words. 8 figures are present in the manuscript. A supplementary file consisting of supplementary methods, supplementary references, 7 figures and 1 table is associated with the manuscript.

Acknowledgement. We thank professor Feng Liu for providing the Tg (*runx1*: EGFP) transgenic line.

Funding. This work was supported by the Shanghai Natural Science Foundation of China (19ZR1431600).

Disclosures. No conflicts of interest to disclose.

Abstract

The ubiquitination or SUMOylation of hematopoietic related factors plays pivotal roles in hematopoiesis. RNF111, known as a ubiquitin ligase (Ubl), is a newly discovered SUMO-targeted ubiquitin ligase (STUbl) involved in multiple signaling pathways mediated by TGF- β family members. However, its role in hematopoiesis remains unclear. Herein, a heritable Rnf111 mutant zebrafish line was generated by CRISPR/Cas9-mediated genome editing. Impaired hematopoietic stem and progenitor cells (HSPC) of definitive hematopoiesis was found in Rnf111 deficient mutants. Ablation of Rnf111 resulted in decreased phosphorylation of Smad2/3 in HSPC. Definitive endoderm 2 inducer (IDE2), which specifically activates TGF- β signaling and downstream Smad2 phosphorylation, can restore the definitive hematopoiesis in Rnf111-deficient embryos. Further molecular mechanism studies revealed that Gcsfr/NO signaling was an important target pathway of Smad2/3 involved in Rnf111-mediated HSPC development. In conclusion, our study demonstrated that Rnf111 contributes to the development of HSPC by maintaining Smad2/3 phosphorylation and the Gcsfr/NO signaling pathway activation.

Keywords: Rnf111, Ubiquitin ligase (Ubl), HSPC, Smad2/3, Gcsfr/NO

Introduction

In vertebrates, hematopoiesis occurs in multiple waves.^{1, 2} The earliest wave, namely primitive hematopoiesis, mainly produces erythroid and myeloid cells.² The second wave of hematopoiesis- the intermediate hematopoiesis-occurs in the posterior blood island (PBI) and emerges erythromyeloid progenitors (EMP).³ The last wave, also called definitive hematopoiesis, generates hematopoietic stem cells (HSC) that are multipotent and can give rise to all lineages of blood cells for the whole life span.⁴ The hematopoietic regulatory network of zebrafish (*Danio rerio*) is highly conserved with that of mammals. Almost all transcription factors and key genes involved in hematopoietic regulation in mammals have orthologues in zebrafish.⁵ In zebrafish, definitive hematopoietic stem and progenitor cells (HSPC) emerge from the ventral wall of the dorsal aorta (VDA) at approximately 33 to 35 hours post-fertilization (hpf), functionally equivalent to mammalian aorta–gonad–mesonephros (AGM),^{6, 7} then the nascent HSPC migrates to the caudal hematopoietic tissue (CHT), which is analogous to the mammalian fetal liver.⁸ Beginning at around 4 days post-fertilization (dpf), HSPC migrates through CHT to the adult hematopoietic tissue-thymus and kidney marrow, which is similar to the process that HSC migrates through fetal liver and homes to bone marrow in mammals.⁸

The development of HSC is precisely regulated by a variety of transcription factors and signaling pathways. Dysregulation of this process leads to serious developmental defects or diseases. And it has been reported that the ubiquitination and SUMOylation of hematopoietic related factors play an important role in hematologic system.⁹⁻¹¹ Arkadia (also known as RING finger 111, RNF111) is a nuclear E3 ubiquitin ligase (UbL) that ubiquitinates intracellular effectors and regulators of TGF- β /Nodal-related signaling, leading to their proteasome-dependent degradation. The characteristic RING finger domain of RNF111 in its C-terminus is required for degradation of the three major negative regulators of TGF- β signaling- Smad7, c-Ski and SnoN- in a SUMO-independent manner.¹²⁻¹⁵ RNF111 specifically regulates induced regulatory T (iTreg) cell differentiation through facilitating the degradation of SKI/SnoN proteins.¹⁶ Knockdown of RNF111 promotes the differentiation of C2C12 myoblasts through reducing Myostatin/TGF-beta signaling.¹⁷ RNF111 is also involved in atrial fibrillation induced myocardial fibrosis through mediating poly-ubiquitination and degradation of Smad7.¹⁸ Besides, RNF111 has been recognized as a SUMO-targeted ubiquitin ligase (STUbL) in the past several years. STUbL recognizes

polysumoylated proteins through N-terminal SUMO-interacting motifs (SIM), mediating the ubiquitination degradation of target sumoylated substrates.¹⁹ RNF111 was shown to ubiquitinate polysumoylated promyelocytic leukemia (PML) in a SIM-dependent manner and was required for subsequent degradation of the polyubiquitinated PML product in promyelocytic leukemia nuclear bodies (PML-NB).^{20,21} Meanwhile, RNF111 has been discovered to enhance the ubiquitylation of SUMOylated xeroderma pigmentosum C (XPC) protein, a pivotal DNA damage recognition factor of nucleotide excision repair (NER), to facilitate the DNA damage response.²² However, the physiological function in hematopoiesis of RNF111 currently remains unknown.

To determine the role of RNF111 in hematopoiesis, we generated a heritable *Rnf111* zebrafish mutant line by CRISPR/Cas9-mediated knockout technology. The *Rnf111*-deficient embryos showed defects in definitive hematopoiesis, manifested by a reduction in HSPC, whereas primitive hematopoiesis was unaffected. Mechanistic studies indicated that *Rnf111* plays an important role in the development of HSPC through maintaining the phosphorylation of Smad2/3 and activating the *Gcsfr*/NO signaling pathway.

Methods

Zebrafish strains maintenance and mutant generation

Zebrafish were maintained and staged under standard conditions as described before.²³ All animal related procedures were approved by the Ethics Committee of Ruijin Hospital Affiliated to Shanghai Jiao Tong University School of Medicine. The methods for generating *Rnf111* knockout zebrafish and identifying the genotypes are described in supplementary methods. Heritable fishes with 4 bases deletion were preserved and utilized for subsequent phenotypic analysis.

Whole-mount in situ hybridization (WISH)

Whole-mount in situ hybridization was carried out with probes including *cmyb*, *scl*, *mpx*, *hbae1*, *runx1* and *rag1* probes, which were previously used and reported before,²⁴ and the *gcsfr*, *rnf111* and *gata2b* probes, which were newly cloned into pGEM-T Easy vector (promega). Details in the procedure are described in supplementary methods.

Morpholinos (MO) and mRNA microinjection

The sequences of MO and details about mRNA microinjection are provided in the supplementary methods.

Quantitative real-time PCR

The procedures of reverse transcription and quantitative PCR are described in supplementary methods. Each sample was tested in triplicate. The supplementary table detailed the primers employed for real-time quantitative PCR (RT-qPCR).

Immunofluorescence assay, Bromodeoxyuridine (BrdU) and enhanced green fluorescent protein (EGFP) double immunostaining and confocal fluorescent imaging

The 3 dpf transgenic Tg (*cmyb:EGFP*)²⁵ embryos were used for immunofluorescence assay. BrdU and EGFP double staining was carried out in the 3 dpf Tg (*runx1:EGFP*)²⁶ and Tg (*cmyb:EGFP*) embryos. Detailed procedures are described in supplementary methods. FV 1000 confocal microscope (Olympus, Tokyo, Japan) was applied for observation and taking images²⁴.

Sudan Black B staining

The embryos were treated with 4% paraformaldehyde (PFA) overnight at 4°C, followed by incubation with Sudan Black (Sigma-Aldrich) solution for 25 minutes. Subsequently, they were thoroughly washed in 70% ethanol to facilitate the detection the granules of granulocytes.

Cell culture and luciferase reporter assay

HEK293T cells were used for plasmid transfections according to the manufacturer's instructions. Detailed procedures are shown in supplementary methods.

Immunohistochemistry

The 3 dpf embryos were used in immunohistochemistry according to procedures in supplementary methods.

Western blot and Chromatin immunoprecipitation PCR (ChIP-PCR)

The preparation of samples, information about antibodies and other relevant details in Western blot analysis and ChIP-PCR are described in supplementary methods.

Chemical treatment

The concentration of drugs and duration of treatments are listed in supplementary methods.

DAF-FM assay

Embryos at 28 hpf, 2 dpf and 3 dpf were exposed to 5 μM DAF-FM DA (4-amino-5-methylamino-2',7'-difluorofluorescein diacetate) for 2 hours in the dark at 28.5 °C, rinsed in fish water and then observed under a fluorescence microscope.²⁷ The NO fluorescence intensity was

quantified by ImageJ software and the relative intensity was calculated and presented by mean \pm S.D.

Statistical analysis

All experiments were independently replicated at least three times. SPSS software (version 20) was used for statistical analysis. Comparisons between two groups were conducted using Student's unpaired two-tailed t-test, while one-way analysis of variance (ANOVA) was employed for comparing multiple groups. Significance was established at a threshold of $P < 0.05$.

Results

Evolutionary conservation of Rnf111 and generation of a heritable Rnf111-mutation zebrafish line

Zebrafish Rnf111 contains all the structural motifs including nuclear localization signals, RING finger domain, Small Ubiquitin-like Modifiers (SUMO)-interacting motifs (SIM) and Axin1 interaction domain (AID), which are originally described for mouse RNF111.²⁸ Zebrafish *rnf111* has a highly degree of synteny with the *RNF111* locus in human (Supplementary Figure S1A) and its protein shares a 53.46% sequence similarity with human RNF111 (Supplementary Figure S1B). Subsequently, both antisense and sense probes were used to detect the mRNA expression pattern of *rnf111* in zebrafish embryos with whole-mount mRNA in situ hybridization (WISH) assay. The results showed that *rnf111* is a maternal gene that exhibits a ubiquitous expression, with high expression in the nervous system and relatively weak expression in hematopoietic tissues (Supplementary Figure S1C), consistent with the single-cell gene expression data on DanioCell website.

To address the roles of Rnf111 in hematopoiesis, a Rnf111 mutant line was generated using the CRISPR/Cas9 system. The target site was in exon 5 and four nucleotides were deleted (Figure 1A, B), which led to a frameshift and formed a truncated protein containing only 552 amino acids (Figure 1C). The wildtype and mutant coding sequence were cloned to PCS2+ vector and transfected to 293T cells respectively, and a shorter protein corresponding to the truncated mutant was detected by western blot analysis (Figure 1D). To further confirm the function of the truncated protein, the CAGA12-luc transcriptional reporter construct,^{15,29} stimulated by TGF- β and activin, was used to test whether the truncated protein can promote TGF- β -inducible DNA elements

activation by dual luciferase reporter assay. As expected, Rnf111 mutants failed to promote the luciferase reporter gene expression (Figure 1E), indicating that the *rnf111* mutated allele was indeed loss-of-function. Meanwhile, we found that the homozygous mutants cannot grow into adult fish and died within 8 to 10 days, which was consistent with *Rnf111* knockout mice.

Ablation of Rnf111 impairs the development of definitive HSPC

We analyzed the hematopoietic phenotypes of Rnf111 mutated embryos. Firstly, a series of markers involved in primitive hematopoiesis, such as hematopoietic precursor cell marker *scl*,³⁰ mature erythrocyte marker *hbae1*³¹ and myeloid-specific marker *mpx*³² were examined at 22 hpf (Supplementary Figure S2A) and no overt changes have been observed, suggesting that primitive hematopoiesis was not affected in Rnf111 mutants. Then WISH analysis of the definitive wave was carried out. The expression of HSPC markers *cmyb*³³ and *runx1*¹ were normal at 36 hpf and the expression of *cmyb* was decreased in Rnf111 mutants from 2 dpf (Figure 2A, B), suggesting the definitive HSPC was impaired. Moreover, the expression of mature erythrocyte marker *hbae1*, myeloid-specific marker *mpx* and Sudan Black staining, and lymphoid specific marker *rag1*³⁴ were all diminished in Rnf111 mutants (Figure 2C), which further indicated that the deficiency of HSPC occurred in the Rnf111 mutants.

To further confirm the phenotype of hematopoiesis, a translation-blocking antisense MO oligonucleotide, which can sharply knockdown the Rnf111 protein level (Supplementary Figure S2B), was used to inhibit the function of Rnf111. The phenotype of both primitive and definitive waves of *rnf111* MO injected embryos (*rnf111* morphants) were detected by WISH using markers for each blood lineage involved in hematopoietic development. In consistence with the results in Rnf111 mutants, the markers *scl*, *mpx* and *hbae1* were normal in primitive hematopoiesis (Supplementary Figure S2C). The expression of definitive HSPC markers *cmyb*³³ and *runx1* in *rnf111* morphants was comparable with wild embryos at 33 hpf (Supplementary Figure S3A, B), which indicated that deficiency of Rnf111 had no effect on the generation of HSPC. The number of HSPC was decreased from 2 dpf until all subsequent developmental stages (Supplementary Figure S3A), suggesting the definitive HSPC was impaired. Then we injected MO to Tg (*cmyb*:EGFP) embryos (a stable zebrafish transgenic line expressing EGFP under the control of the *cmyb* promoter).²⁵ As expected, the number of EGFP-positive cells was significantly decreased in the CHT at 2 dpf and 3 dpf (Supplementary Figure S3C). Finally, the markers of downstream

lineages were all diminished in *rnf111* morphants (Supplementary Figure S3D). These results further confirmed the HSPC was specifically affected in Rnf111 deficient embryos.

The functional domain of ubiquitin ligase is required for Rnf111 to regulate HSPC development

Rnf111 is a multifunctional protein acting as both ubiquitin ligase (UbL) and SUMO-targeted ubiquitin ligase (STUbL). In order to elucidate the functional contribution of Rnf111 in the regulation of HSPC development, four vectors-Rnf111 WT, Rnf111 SIM MU, Rnf111 RING MU and Rnf111 -4bp MU were constructed and rescue effects of corresponding mRNA on HSPC defects were compared in Rnf111 deficient embryos (Figure 3A). The amino acids of the three SUMO-interacting motifs (SIM) were all mutated to alanine in Rnf111 SIM mutant (Rnf111 SIM MU), which abolishes its binding to SUMO-modified substrates.²¹ Four cysteine residues within the RING domain of the active center of the ubiquitin ligase activity were mutated in Rnf111 RING mutant (Rnf111 RING MU), which enables it to still bind to but not to degrade the substrates.¹⁵ The result showed that Rnf111 WT effectively rescued the deficient HSPC in Rnf111 mutants, while the mRNA, whose sequence was consistent with the sequence of Rnf111 -4bp mutant line (-4bp MU), failed (Figure 3B), demonstrating that the phenotype observed in Rnf111 mutants was indeed Rnf111 dependent. Interestingly, while Rnf111 SIM MU could rescue the defect of HSPC, Rnf111 RING MU lost its rescue effect (Figure 3B). The same rescue assays were carried out in *rnf111* morphants, and the similar results were obtained (Supplementary Figure S4A, B, C). All these results suggested that Rnf111 regulates HSPC development depending on its UbL function rather than the STUbL one.

Decreased proliferation capacity of HSPC was observed in *rnf111* morphants

TGF- β signaling, which was the main pathway that Rnf111 regulated,¹²⁻¹⁵ can affect HSPC development by regulating proliferation.^{35,36} Therefore, Brdu incorporation assay was carried out to detect the proliferation ability of HSPC in Tg (*runx1*: EGFP) and Tg (*cmyb*: EGFP) *rnf111* morphants. The results showed that the number of the Brdu⁺/GFP⁺ cells in both transgenic lines was sharply decreased in the CHT region of *rnf111* morphants (Figure 4A, B, Supplementary Figure S4D), indicating that the proliferation capacity of HSPC was severely impaired, which may be related to impaired TGF- β signaling.

The decrease of p-Smad2/3 protein leads to HSPC defect in Rnf111 deficient embryos

In line with our finding that Rnf111 regulated the development of HSPC depending on its UbL function, it was reported previously that this function was also required for Rnf111 to regulate TGF- β signaling pathway. Rnf111 degrades Smad7, an inhibitory protein of TGF- β signaling pathway, in a SUMO-independent manner and promotes the phosphorylation of receptor- Smads (Smad2 and Smad3). It is also reported that TGF- β at low doses (picogram levels) stimulated the colony formation from CD34⁺ cells.³⁶ Considering the reduced proliferation capacity of HSPC observed in *rnf111* morphants, we speculated that Rnf111 may regulate the development of HSPC by affecting the phosphorylation of Smad2/3. Therefore, the anti-p-Smad2/3 and EGFP double immunostaining assay were performed in Tg (*cmyb*: EGFP) embryos. The result showed a basal level of Smad2/3 phosphorylation was detected in HSPC of wild type embryos (Figure 5A, A', A''), while it was significantly reduced in HSPC of *rnf111* morphants (Figure 5B, B', B'', C). Immunohistochemistry and western blot analysis of whole embryo demonstrated the same downward trend of p-Smad2/3 (Figure 5D, E, F) with no obvious changes in general Smad2 and Smad3 protein levels. Meanwhile, the protein level of Smad7 was up-regulated (Figure 5G), which may be responsible for the reduction of p-Smad2/3. Then, to further investigate whether the observed Rnf111 ablation caused HSPC defective phenotype was due to the decrease of p-Smad2/3, definitive endoderm 2 inducer (IDE2), a drug specifically activates TGF- β signaling and downstream Smad2 phosphorylation with no effect on hemogenic endothelium (HE) and HSPC emergence (Supplementary Figure S5A, B), was used to treat Rnf111 mutants. As expected, IDE2 effectively rescued *cmyb* expression (Figure 5H). We also carried the IDE2 rescue assay in *rnf111* morphants, the same result was obtained (Supplementary Figure S5C, D). All these results demonstrated that the reduction of p-Smad2/3 was the key cause for HSPC defect in Rnf111 deficient embryos.

Gcsf signaling pathway was the downstream target of Rnf111-Smad2/3

As an important regulator of classical TGF- β signaling pathway, Rnf111 promotes TGF- β signaling by degrading the repressor proteins and facilitates the phosphorylation of receptor-Smad2/3. It has been reported that TGF- β can regulate the amount of Granulocyte-macrophage colony-stimulating factor receptors (GM-CSFR), interleukin-3 receptors (IL-3R), and granulocyte colony-stimulating factor receptors (GCSFR) in mouse hematopoietic progenitor cell lines without affecting the receptor affinity.³⁷ Gcsf signaling is required for HSPC emergence and expansion in

zebrafish.³⁸ Based on our results, we hypothesized that Rnf111 regulates phosphorylation of Smad2/3 to promote Gcsf signaling in HSPC development. To test this hypothesis, quantitative RT-PCR was performed to detect the expression of *gcsfr*, *gcsfa* and *gcsfb* in 3 dpf embryos. All these three genes exhibited decreased expression in Rnf111 mutants and *rnf111* morphants (Figure 6A, Supplementary Figure S6A). The WISH results further confirmed that *gcsfr* expression was reduced (Figure 6B). However, the expressions of *gcsfr* in Rnf111 mutants (36 hpf) and AGM region of *rnf111* morphants (31 hpf) were unchanged (Supplementary Figure S6B, C). Then, *cmvb*-GFP positive HSPC at 3 dpf were sorted to detect *gcsfr* expression with quantitative RT-PCR assay. The result showed that *gcsfr* expression was reduced in HSPC (Figure 6C).

Then the -2.5k promoter sequence of *gcsfr* was cloned into the PGL3-basic vector and luciferase activity assay was performed. The results indicated that IDE2, Rnf111 WT and Rnf111 SIM MU could activate the luciferase expression, while Rnf111 RING MU failed (Figure 6D). These results were in line with the *in vivo* rescue assay (Figure 3). Then, GFP and Smad2-GFP RNA were injected in zebrafish embryos respectively and chromatin immunoprecipitation PCR (ChIP-PCR) analysis was carried out to detect the binding ability of Smad2 to endogenous *gcsfr* promoter. The results showed that the promoter region of *gcsfr* could be specifically co-immunoprecipitated with Smad2-GFP (Figure 6E).

In order to further confirm the pivotal role of Gcsf signaling in Rnf111 regulation of HSPC development, the RNA rescue assay of both ligand (*Gcsfb*) and receptor (*Gcsfr*) was implemented. As expected, both *gcsfb* and *gcsfr* RNA rescued the developmental defects of HSPC in both Rnf111 mutants and *rnf111* morphants (Figure 6F, Supplementary Figure S6D, F). Moreover, when the expression of *Gcsfr* was knocked down by *gcsfr* MO, the rescue effect of IDE2 was abolished (Supplementary Figure S6E, F), suggesting that *Gcsfr* was a pivotal target of Smad2.

Decreased Gcsfr-Nitric Oxide (NO) signaling leads to the defect of HSPC development in Rnf111 deficient embryos

It was reported that infection-induced Gcsfr-NO signaling can enhance the expansion of HSPC in zebrafish and *Cebpb*-*Nos2a* acts downstream of Gcsf signaling.³⁹ To verify whether *Cebpb* is involved in HSPC defect induced by Rnf111 deficiency, *cebpb* RNA was injected into the Rnf111 mutants. Noticeably, the defect of HSPC could be effectively rescued (Figure 7A). Since our RT-qPCR results revealed decreased expression of the downstream gene *nos2a* (*inosa*)

both in Rnf111 mutants (2 dpf and 3 dpf) and *rnf111* morphants (3 dpf) (Figure 7B, Supplementary Figure S7A), the cell-permeable 4-amino-5-methylamino-2',7'-difluorescein diacetate (DAF-FM DA) fluorescent NO probe was used to examine the active NO production.⁴⁰ The results showed that NO production was decreased in *rnf111* morphants at 2 dpf and 3 dpf (Figure 7C, D). It is reported that blood flow-induced Klf2a-NO signaling can regulate NO production.²⁷ Therefore, we detected the expression of *klf2a* in Rnf111 deficient embryos by WISH assay and quantitative RT-PCR assay. *klf2a* expression was not decreased in Rnf111 deficient embryos compared to control ones (Supplementary Figure S7B, C), suggesting that Klf2a-NO signaling did not contribute to the defects of HSPC in Rnf111 deficient embryos. In addition, we also employed the rescue assay by treating Rnf111 mutants and *rnf111* morphants with NO agonist, S nitroso N-acetylpenicillamine (SNAP). The WISH results showed that the expression of *cmyb* was partially restored (Figure 7E, Supplementary Figure S7D). And the rescue effect of SNAP was also proved in Tg(*cmyb*:EGFP) line (Supplementary Figure S7F). Next, we used the NOS2-specific inhibitor 1400W to block the production of NO and found that the rescue effect of *gcsfr* RNA on HSPC was abolished (Supplementary Figure S7E, F). Taken together, these data suggested that Rnf111 regulates HSPC expansion, at least in part, through Gcsfr-Cebpb-NO signaling.

Discussion

RNF111 was a ubiquitin ligase that enhances TGF- β signaling by promoting the degradation of repressors (SnoN, Ski and Smad7) that inhibit the expression of target genes.^{13,14} RNF111 also was the second SUMO-targeting ubiquitin ligase (STUbL) identified, which targets substrates with SUMO1-capped SUMO2 chains significantly superior to other identical substrates with homogeneous SUMO2 or SUMO1 chains.²¹ Rnf111 was responsible for induction of the node through enhancing the nodal signaling,^{41,42} as well as progression of tissue fibrosis and cancer through regulating the TGF- β signaling.⁴³⁻⁴⁵ In this study, we found the novel biological role of Rnf111 in zebrafish hematopoiesis. Both Rnf111 mutants and *rnf111* morphants showed impaired definitive hematopoiesis without defects in primitive wave, manifested by a decrease of definitive HSPC and downstream lineages. Although we could not exclude the possibility that EMP partially contributed to decreased *mpx* expression and Sudan Black staining in mutants at 2 dpf, the number

of myeloid cells of HSPC origin was indeed reduced, presented by reduced *mpx* expression and Sudan Black staining in Rnf111 mutants and *rnf111* morphants at 2 dpf, 3 dpf, and 4 dpf. The homozygous mutants died within 8 to 10 days, which was consistent with the recessive lethal results in *Rnf111* gene-trap insertion mutation mice.⁴² And the regulatory role of Rnf111 in HSPC development depends on its UbL function rather than STUbL one. Our mechanism studies unraveled that the decrease of p-Smad2/3 due to stabilization of Smad7 protein caused by Rnf111 deletion was involved in the developmental defect of HSPC and the decrease of downstream Gcsfr/NO signaling results in an attenuated proliferative ability of HSPC (Figure 8).

The behavior of HSPC such as self-renewal and quiescence is determined by a huge variety of factors, including external signaling cues present in the microenvironment of bone marrow. In the hematopoietic system, TGF- β signaling controls a wide range of biological processes, from immune system homeostasis to hematopoietic stem cell dormancy and self-renewal.⁴⁶ The effect of TGF- β on HSC is bidirectional, with high levels of TGF- β blocking proliferation and low levels of TGF- β promoting proliferation.^{36,47} It is also reported that TGF- β at the dose of 0.01 ng/ml can expand normal HSC, and the phosphorylated Smad2/3 may contribute to this proliferative response of HSC under low concentrations of TGF- β .⁴⁸ Therefore, during the development of normal HSC, appropriate TGF- β concentration is required to maintain the quiescence, self-renewal and differentiation functions. A suitable phosphorylation level of Smad2/3 in HSC is crucial for the maintenance of their normal function in response to the stimulation of low levels of TGF- β . Consistently, our results demonstrated that basal levels of Smad2/3 phosphorylation are present in the HSPC of wild-type embryos (Figure 5 A, A', A'', B, B', B''). However, the p-Smad2/3 was down-regulated in HSPC of *rnf111* morphants, which may be the main cause leading to HSPC defect. The Brdu incorporation assay showed the proliferative ability of HSPC in *rnf111* morphants was decreased compared with WT embryos (Figure 4), indicating that the proliferative response of HSPC to normal concentrations of TGF- β was impaired under the absence of Rnf111, most likely due to the reduction of downstream effector p-Smad2/3. Rescue assay of IDE2 confirmed this notion. These data suggested that Rnf111 is present to maintain HSPC in response to TGF- β signals at normal concentrations.

It has been reported that TGF- β can regulate the amount of GM-CSFR, IL-3R, and GCSFR in mouse hematopoietic progenitor cell lines without significant changes in receptor affinity³⁷. It is

also known that Gcsf signaling promotes the expansion of HSPC in zebrafish embryos³⁸. Indeed, we did find the expression of *gcsfr* was down-regulated in Rnf111 mutants and morphants at 3 dpf, but unchanged in Rnf111 mutants at 36 hpf and AGM region of *rnf111* morphants at 31 hpf (Figure S6B, C). This may be responsible for the unaffected generation and impaired proliferation of HSPC in Rnf111 deficient embryos. Meanwhile, the HSPC defect could be rescued by *gcsfb* and *gcsfr* RNA. Luciferase reporter assay and ChIP-qPCR further confirmed the direct binding of p-Smad2 on *gcsfr* promoter. The rescue effect of IDE2 was blocked by *gcsfr* MO, further confirming that Gcsfr was the target of Smad2/3.

Further experiments confirmed Cebpb/NO pathway was involved in the downstream of Gcsf signaling, evidenced by the rescue effect of *cebpb* RNA and NO donor, and the blocking of the rescue effect of *gcsfr* RNA by NOS2-specific inhibitor 1400W. It was worth noting that NO signaling at earlier developmental stage was not decreased, represented by relatively normal DAF-FM signal intensity at 28 hpf in *rnf111* morphants and *nos2a* expression level at 36 hpf in Rnf111 mutants. However, both DAF-FM signal intensity and *nos2a* expression level were significantly reduced at 2 dpf and 3 dpf (Figure 7B, C, D, Supplementary Figure S7A), which was consistent with the pattern of HSPC reduction in Rnf111-deficient embryos. The proliferation defect of HSPC caused by decreased NO in Rnf111 deficient embryos was consistent with the reported function of NO on HSPC proliferation at physiological concentration,⁴⁹ which further confirmed the pivotal role of NO in Rnf111 regulation of HSPC development. Taken together, we revealed a fine-tuned regulation of HSPC development by ubiquitin ligase.

References

1. Jagannathan-Bogdan M, Zon LI. Hematopoiesis. *Development*. 2013;140(12):2463-2467.
2. Chen AT, Zon LI. Zebrafish blood stem cells. *J Cell Biochem*. 2009;108(1):35-42.
3. Bertrand JY, Kim AD, Violette EP, Stachura DL, Cisson JL, Traver D. Definitive hematopoiesis initiates through a committed erythromyeloid progenitor in the zebrafish embryo. *Development*. 2007;134(23):4147-4156.
4. Orkin SH, Zon LI. Hematopoiesis: an evolving paradigm for stem cell biology. *Cell*. 2008;132(4):631-644.
5. Song HD, Sun XJ, Deng M, et al. Hematopoietic gene expression profile in zebrafish kidney marrow. *Proc Natl Acad Sci U S A*. 2004;101(46):16240-16245.
6. Kissa K, Herbomel P. Blood stem cells emerge from aortic endothelium by a novel type of cell transition. *Nature*. 2010;464(7285):112-115.
7. Kissa K, Murayama E, Zapata A, et al. Live imaging of emerging hematopoietic stem cells and early thymus colonization. *Blood*. 2008;111(3):1147-1156.
8. Murayama E, Kissa K, Zapata A, et al. Tracing hematopoietic precursor migration to successive hematopoietic organs during zebrafish development. *Immunity*. 2006;25(6):963-975.
9. Yu L, Ji W, Zhang H, et al. SENP1-mediated GATA1 deSUMOylation is critical for definitive erythropoiesis. *J Exp Med*. 2010;207(6):1183-1195.
10. Yuan H, Zhou J, Deng M, et al. Sumoylation of CCAAT/enhancer-binding protein alpha promotes the biased primitive hematopoiesis of zebrafish. *Blood*. 2011;117(26):7014-

7020.

11. Yuan H, Zhang T, Liu X, et al. Sumoylation of CCAAT/enhancer-binding protein alpha is implicated in hematopoietic stem/progenitor cell development through regulating runx1 in zebrafish. *Sci Rep.* 2015;5:9011.

12. Mavrakis KJ, Andrew RL, Lee KL, et al. Arkadia enhances Nodal/TGF-beta signaling by coupling phospho-Smad2/3 activity and turnover. *PLoS Biol.* 2007;5(3):e67.

13. Koinuma D, Shinozaki M, Komuro A, et al. Arkadia amplifies TGF-beta superfamily signalling through degradation of Smad7. *EMBO J.* 2003;22(24):6458-6470.

14. Nagano Y, Mavrakis KJ, Lee KL, et al. Arkadia induces degradation of SnoN and c-Ski to enhance transforming growth factor-beta signaling. *J Biol Chem.* 2007;282(28):20492-20501.

15. Levy L, Howell M, Das D, Harkin S, Episkopou V, Hill CS. Arkadia activates Smad3/Smad4-dependent transcription by triggering signal-induced SnoN degradation. *Mol Cell Biol.* 2007;27(17):6068-6083.

16. Xu H, Wu L, Nguyen HH, et al. Arkadia-SKI/SnoN signaling differentially regulates TGF-beta-induced iTreg and Th17 cell differentiation. *J Exp Med.* 2021;218(11):e20210777.

17. Yuzawa H, Koinuma D, Maeda S, Yamamoto K, Miyazawa K, Imamura T. Arkadia represses the expression of myoblast differentiation markers through degradation of Ski and the Ski-bound Smad complex in C2C12 myoblasts. *Bone.* 2009;44(1):53-60.

18. He X, Gao X, Peng L, et al. Atrial fibrillation induces myocardial fibrosis through angiotensin II type 1 receptor-specific Arkadia-mediated downregulation of Smad7. *Circ Res.* 2011;108(2):164-175.

19. Sriramachandran AM, Dohmen RJ. SUMO-targeted ubiquitin ligases. *Biochim Biophys Acta*. 2014;1843(1):75-85.
20. Erker Y, Neyret-Kahn H, Seeler JS, Dejean A, Atfi A, Levy L. Arkadia, a novel SUMO-targeted ubiquitin ligase involved in PML degradation. *Mol Cell Biol*. 2013;33(11):2163-2177.
21. Sriramachandran AM, Meyer-Teschendorf K, Pabst S, et al. Arkadia/RNF111 is a SUMO-targeted ubiquitin ligase with preference for substrates marked with SUMO1-capped SUMO2/3 chain. *Nat Commun*. 2019;10(1):3678.
22. Poulsen SL, Hansen RK, Wagner SA, et al. RNF111/Arkadia is a SUMO-targeted ubiquitin ligase that facilitates the DNA damage response. *J Cell Biol*. 2013;201(6):797-807.
23. Kimmel CB, Ballard WW, Kimmel SR, Ullmann B, Schilling TF. Stages of embryonic development of the zebrafish. *Dev Dyn*. 1995;203(3):253-310.
24. Liu X, Jia X, Yuan H, et al. DNA methyltransferase 1 functions through C/ebpa to maintain hematopoietic stem and progenitor cells in zebrafish. *J Hematol Oncol*. 2015;8:15.
25. North TE, Goessling W, Walkley CR, et al. Prostaglandin E2 regulates vertebrate haematopoietic stem cell homeostasis. *Nature*. 2007;447(7147):1007-1011.
26. Zhang P, He Q, Chen D, et al. G protein-coupled receptor 183 facilitates endothelial-to-hematopoietic transition via Notch1 inhibition. *Cell Res*. 2015;25(10):1093-1107.
27. Wang L, Zhang P, Wei Y, Gao Y, Patient R, Liu F. A blood flow-dependent klf2a-NO signaling cascade is required for stabilization of hematopoietic stem cell programming in zebrafish embryos. *Blood*. 2011;118(15):4102-4110.
28. Bessarab DA, Mathavan S, Jones CM, Ray Dunn N. Zebrafish Rnf111 is encoded

by multiple transcripts and is required for epiboly progression and prechordal plate development. *Differentiation*. 2015;89(1-2):22-30.

29. Denkler S, Itoh S, Vivien D, ten Dijke P, Huet S, Gauthier JM. Direct binding of Smad3 and Smad4 to critical TGF beta-inducible elements in the promoter of human plasminogen activator inhibitor-type 1 gene. *EMBO J*. 1998;17(11):3091-3100.

30. Dooley KA, Davidson AJ, Zon LI. Zebrafish scl functions independently in hematopoietic and endothelial development. *Dev Biol*. 2005;277(2):522-536.

31. Brownlie A, Hersey C, Oates AC, et al. Characterization of embryonic globin genes of the zebrafish. *Dev Biol*. 2003;255(1):48-61.

32. Lieschke GJ, Oates AC, Crowhurst MO, Ward AC, Layton JE. Morphologic and functional characterization of granulocytes and macrophages in embryonic and adult zebrafish. *Blood*. 2001;98(10):3087-3096.

33. Thompson MA, Ransom DG, Pratt SJ, et al. The cloche and spadetail genes differentially affect hematopoiesis and vasculogenesis. *Dev Biol*. 1998;197(2):248-269.

34. Willett CE, Cherry JJ, Steiner LA. Characterization and expression of the recombination activating genes (rag1 and rag2) of zebrafish. *Immunogenetics*. 1997;45(6):394-404.

35. Sitnicka E, Ruscetti FW, Priestley GV, Wolf NS, Bartelmez SH. Transforming growth factor beta 1 directly and reversibly inhibits the initial cell divisions of long-term repopulating hematopoietic stem cells. *Blood*. 1996;88(1):82-88.

36. Kale VP. Differential activation of MAPK signaling pathways by TGF-beta1 forms the molecular mechanism behind its dose-dependent bidirectional effects on hematopoiesis.

Stem Cells Dev. 2004;13(1):27-38.

37. Jacobsen SE, Ruscetti FW, Dubois CM, Lee J, Boone TC, Keller JR. Transforming growth factor-beta trans-modulates the expression of colony stimulating factor receptors on murine hematopoietic progenitor cell lines. *Blood*. 1991;77(8):1706-1716.

38. Stachura DL, Svoboda O, Campbell CA, et al. The zebrafish granulocyte colony-stimulating factors (Gcsfs): 2 paralogous cytokines and their roles in hematopoietic development and maintenance. *Blood*. 2013;122(24):3918-3928.

39. Hall CJ, Flores MV, Oehlers SH, et al. Infection-responsive expansion of the hematopoietic stem and progenitor cell compartment in zebrafish is dependent upon inducible nitric oxide. *Cell Stem Cell*. 2012;10(2):198-209.

40. North TE, Goessling W, Peeters M, et al. Hematopoietic stem cell development is dependent on blood flow. *Cell*. 2009;137(4):736-748.

41. Niederlander C, Walsh JJ, Episkopou V, Jones CM. Arkadia enhances nodal-related signalling to induce mesendoderm. *Nature*. 2001;410(6830):830-834.

42. Episkopou V, Arkell R, Timmons PM, Walsh JJ, Andrew RL, Swan D. Induction of the mammalian node requires Arkadia function in the extraembryonic lineages. *Nature*. 2001;410(6830):825-830.

43. Liu FY, Li XZ, Peng YM, Liu H, Liu YH. Arkadia-Smad7-mediated positive regulation of TGF-beta signaling in a rat model of tubulointerstitial fibrosis. *Am J Nephrol*. 2007;27(2):176-183.

44. Le Scolan E, Zhu Q, Wang L, et al. Transforming growth factor-beta suppresses the ability of Ski to inhibit tumor metastasis by inducing its degradation. *Cancer Res*.

2008;68(9):3277-3285.

45. Nagano Y, Koinuma D, Miyazawa K, Miyazono K. Context-dependent regulation of the expression of c-Ski protein by Arkadia in human cancer cells. *J Biochem.* 2010;147(4):545-554.

46. Blank U, Karlsson S. TGF-beta signaling in the control of hematopoietic stem cells. *Blood.* 2015;125(23):3542-3550.

47. Kale VP, Vaidya AA. Molecular mechanisms behind the dose-dependent differential activation of MAPK pathways induced by transforming growth factor-beta1 in hematopoietic cells. *Stem Cells Dev.* 2004;13(5):536-547.

48. Park SM, Deering RP, Lu Y, et al. Musashi-2 controls cell fate, lineage bias, and TGF-beta signaling in HSCs. *J Exp Med.* 2014;211(1):71-87.

49. Hummer J, Kraus S, Brandle K, Lee-Thedieck C. Nitric Oxide in the Control of the in vitro Proliferation and Differentiation of Human Hematopoietic Stem and Progenitor Cells. *Front Cell Dev Biol.* 2020;8:610369.

Figure 1. *The generation of Rnf111 mutant line. (A) The Cas9 target site was in the fifth exon and 4bp nucleotides were deleted. (B) The sequencing peak maps of wildtype and mutant. (C) Schematic representation of wild-type and mutant Rnf111 proteins. (D) Western blot of HA-tagged wild type and mutant Rnf111 proteins expressed in HEK293T cells. (E) CAGA12-luciferase transcriptional reporter assay of wildtype and mutant Rnf111. The data are presented as mean \pm S.D. with $**P < 0.01$. WT: wildtype; MU: Rnf111 mutants with deletion of 4bp nucleotides; SIM: SUMO-interacting motifs; bp: base pair.

Figure 2.* Impairment of definitive hematopoiesis in Rnf111 mutants. (A) WISH analysis of *cmyb* expression from 36 hpf to 8 dpf. (B) WISH assay of *runx1* in mutants at 36 hpf. (C) WISH analysis of key hematopoietic markers and Sudan Black analysis. All experiments were independently replicated at least three times. MU: Rnf111 mutants with deletion of 4bp nucleotides; hpf: hours post-fertilization; dpf: days post-fertilization; WISH: whole-mount in situ hybridization.

Figure 3.* Schematic representation and rescue assay of the four Rnf111 constructs. (A) Schematic diagram of Rnf111 WT, Rnf111 RING mutant, Rnf111 SIM mutant and -4bp mutant protein. (B) WISH analysis of rescue efficiency of Rnf111 WT, Rnf111 RING mutant, Rnf111 SIM mutant and Rnf111 -4bp mutant RNA. Red arrows indicate *cmyb*-positive HSPC. All experiments were independently replicated at least three times. WT: wildtype; RING MU: Rnf111 RING mutant with the RING domain mutated; SIM MU: Rnf111 SIM mutant with three SUMO-interacting motifs all mutated; SIM: SUMO-interacting motifs; -4bp MU: Rnf111 -4bp mutant with deletion of 4bp nucleotides; dpf: days post-fertilization; MU: Rnf111 mutants with deletion of 4bp nucleotides; WISH: whole-mount in situ hybridization.

Figure 4.* Brdu incorporation assay. (A) Double immunostaining of *runx1*-EGFP and anti-Brdu in the CHT of Tg (*runx1*-EGFP) line at 3 dpf. White arrows indicate Brdu and *runx1*-EGFP double positive cells. (B) Statistics of Brdu and *runx1*-EGFP double positive cells. The data are presented

as mean \pm S.D. with $**P < 0.01$. Tg: transgenic; EGFP: enhanced green fluorescent protein; dpf: days post-fertilization; WT: wildtype; MO *rnf111*: *rnf111* morphants; GFP: green fluorescent protein; Brdu: Bromodeoxyuridine; CHT: caudal hematopoietic tissue.

Figure 5.* Analysis of p-Smad2/3, Smad7 and IDE2 rescue assay in Rnf111 deficient embryos.

(A, A', A'', B, B', B'') Double immunostaining of anti-GFP (A, B) and anti-p-Smad2/3 (A', B') in the CHT of Tg (*cmyb*-EGFP) line at 3 dpf. The bottom panel shows merged images (A'', B''). White arrows indicate p-Smad2/3 and *cmyb*-EGFP double positive cells. (C) Statistics of p-Smad2/3 and *cmyb*-EGFP double positive cells. The data are presented as mean \pm S.D. with $***P < 0.001$. (D, E) Immunohistochemistry of p-Smad2/3. (F) Western blot analysis of p-Smad2, Smad2, p-Smad3 and Smad3. (G) Western blot analysis of Smad7. (H) WISH analysis of rescue efficiency of IDE2. Red arrows indicate *cmyb*-positive HSPC in the CHT. All experiments were independently replicated at least three times. WT: wildtype; MO *rnf111*: *rnf111* morphants; GFP: green fluorescent protein; MU: Rnf111 mutants with deletion of 4bp nucleotides; IDE2: definitive endoderm 2 inducer; CHT: caudal hematopoietic tissue; Tg: transgenic; EGFP: enhanced green fluorescent protein; hpf: hours post-fertilization; WISH: whole-mount in situ hybridization; HSPC: hematopoietic stem and progenitor cell.

Figure 6.* Gcsf signaling was the downstream target of Rnf111-Smad2/3.

(A) RT-qPCR of *gcsfa*, *gcsfb* and *gcsfr* in siblings and mutants at 3 dpf. The data are presented as mean \pm S.D. with $*P < 0.05$, $**P < 0.01$. (B) WISH analysis of *gcsfr*. (C) RT-qPCR of *gcsfr* in HSPC of *rnf111* morphants. The data are presented as mean \pm S.D. with $***P < 0.01$. (D) Luciferase assay of *gcsfr* promotor in HEK293T cells. The data are presented as mean \pm S.D. with $*P < 0.05$, $**P < 0.01$, $***P < 0.001$ and n.s.: no significant difference. (E) ChIP-qPCR assay of Smad2-GFP binding to *gcsfr* promotor at 2 dpf. The data are presented as mean \pm S.D. with $*P < 0.05$ and n.s.: no significant difference. (F) Rescue assay of *gcsfb* and *gcsfr* RNA in Rnf111 mutants. Red arrows indicate *cmyb*-positive HSPC in the CHT. All experiments were independently replicated at least three times. WT: wildtype; MO *rnf111*: *rnf111* morphants; HSPC: hematopoietic stem and progenitor cell; IDE2: definitive endoderm 2 inducer; RING MU: Rnf111 RING mutant with the RING domain mutated; SIM MU: Rnf111 SIM mutant with three SUMO-interacting motifs all

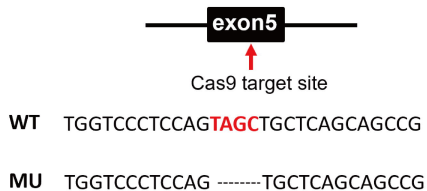
mutated; GFP: green fluorescent protein; MU: Rnf111 mutants with deletion of 4bp nucleotides; RT-qPCR: real-time quantitative polymerase chain reaction; dpf: days post-fertilization; WISH: whole-mount in situ hybridization; ChIP-qPCR: chromatin immunoprecipitation quantitative polymerase chain reaction; CHT: caudal hematopoietic tissue.

Figure 7.* Cebpb-Nos2a acts downstream of Gcsf signaling. (A) Rescue assay of *cebpb* RNA. (B) RT-qPCR result of *inosa* in Rnf111 mutants compared with WT embryos at 36 hpf, 2 dpf and 3 dpf. The data are presented as mean \pm S.D. with $^{**}P < 0.01$ and n.s.: no significant difference. (C) DAF-FM assay showed the decreased production of NO in *rnf111* morphants at 2 dpf and 3 dpf. (D) Statistics of NO fluorescence intensity. The data are presented as mean \pm S.D. with $^{**}P < 0.01$, $^{***}P < 0.001$ and n.s.: no significant difference. (E) Rescue effect of NO agonist SNAP on *cmyb* expression was observed in Rnf111 mutants. Red arrows indicate *cmyb*-positive HSPC in the CHT. All experiments were independently replicated at least three times. dpf: days post-fertilization; MU: Rnf111 mutants with deletion of 4bp nucleotides; hpf: hours post-fertilization; WT: wildtype; MO *rnf111*: *rnf111* morphants; DAF-FM: 4-amino-5-methylamino-2',7'-difluorofluorescein diacetate; SNAP: S nitroso N-acetylpenicillamine; RT-qPCR: real-time quantitative polymerase chain reaction; HSPC: hematopoietic stem and progenitor cell; CHT: caudal hematopoietic tissue.

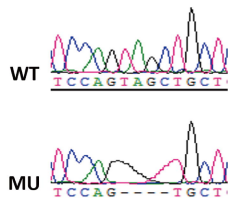
Figure 8.* Schema of Rnf111 regulating the development of hematopoietic stem and progenitor cells by maintaining Smad2/3 phosphorylation and activating Gcsfr/NO signaling pathway. (left) At physiological concentration of TGF- β , ARK/Rnf111 maintains Smad2/3 phosphorylation by promoting the degradation of Smad7 and further facilitates the Gcsfr/NO signaling pathway activation to ensure the proliferative response of HSPC to TGF- β . (right) Deletion of ARK/Rnf111 in HSPC leads to a weakening of TGF- β signaling output, which is manifested by a decrease in Gcsfr/NO signal, resulting in an attenuated proliferative response of HSPC to TGF- β . UbL: ubiquitin ligase; HSPC: hematopoietic stem and progenitor cell.

Figure 1

A



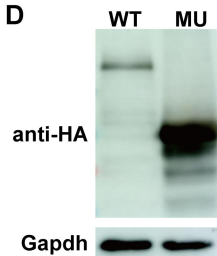
B



C



D



E

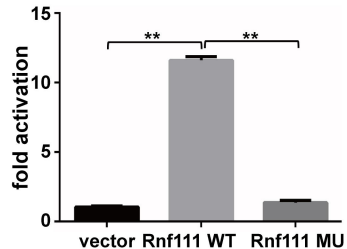
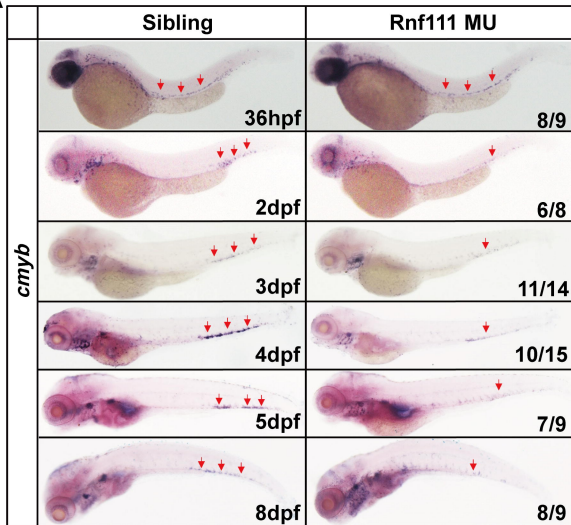
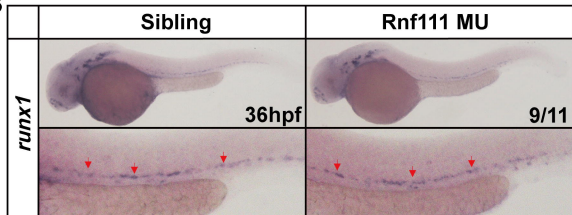


Figure 2

A



B



C

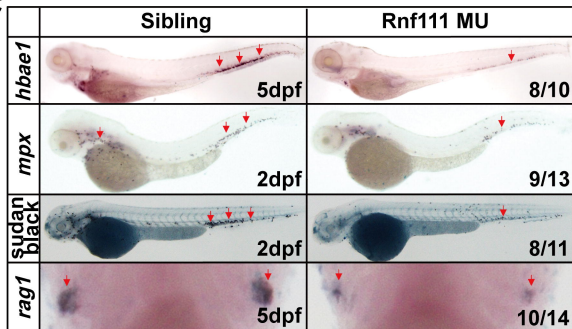


Figure 3

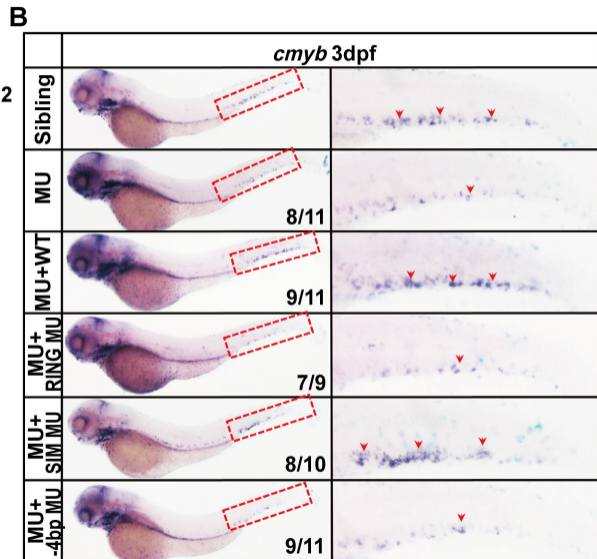
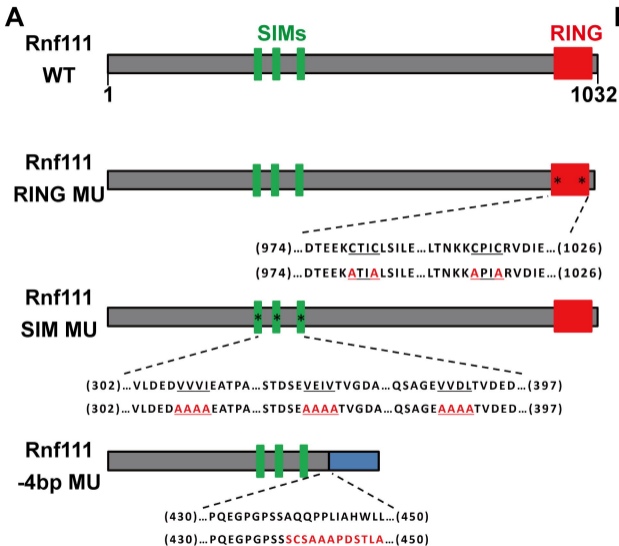
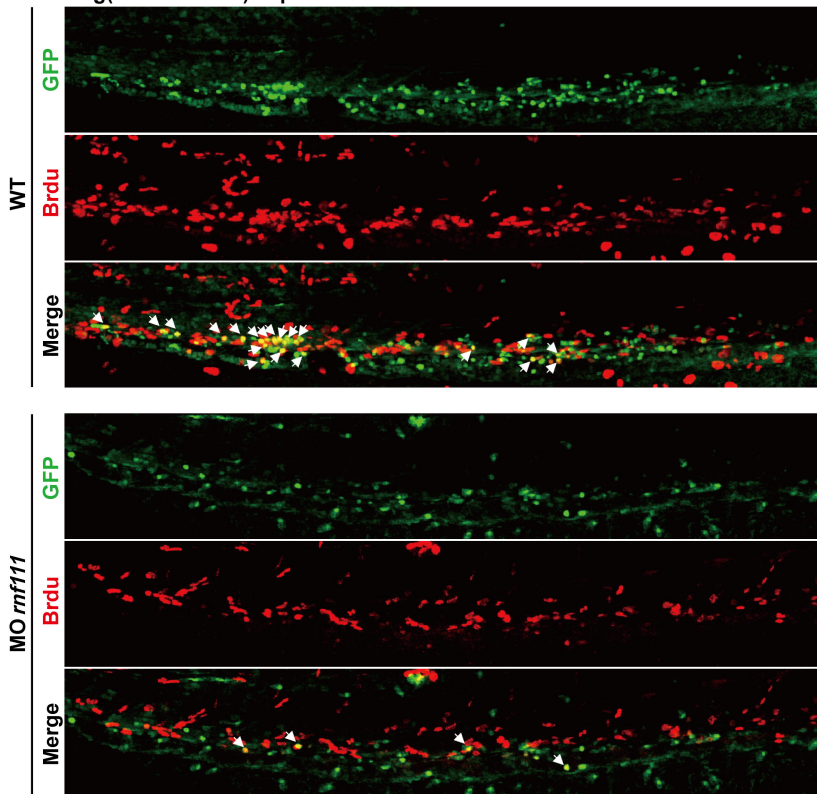


Figure 4

A

Tg(*runx1*:EGFP) 3dpf



B

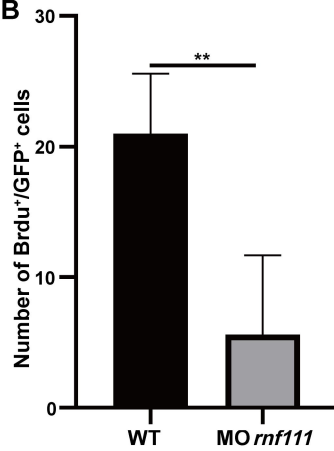


Figure 5

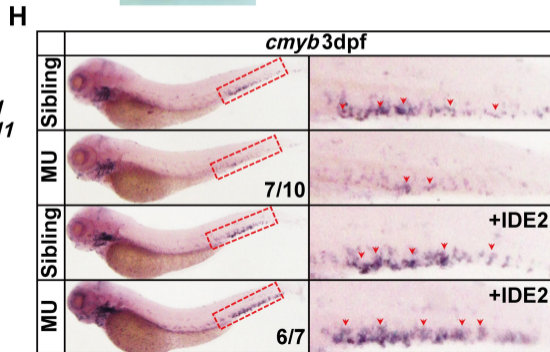
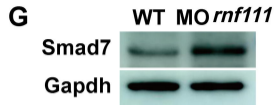
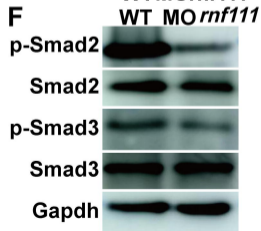
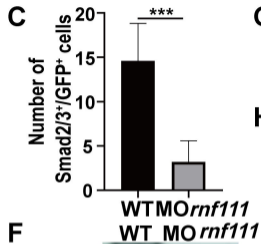
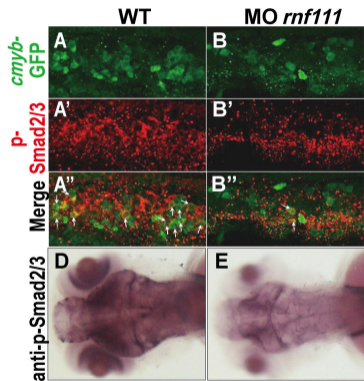


Figure 6

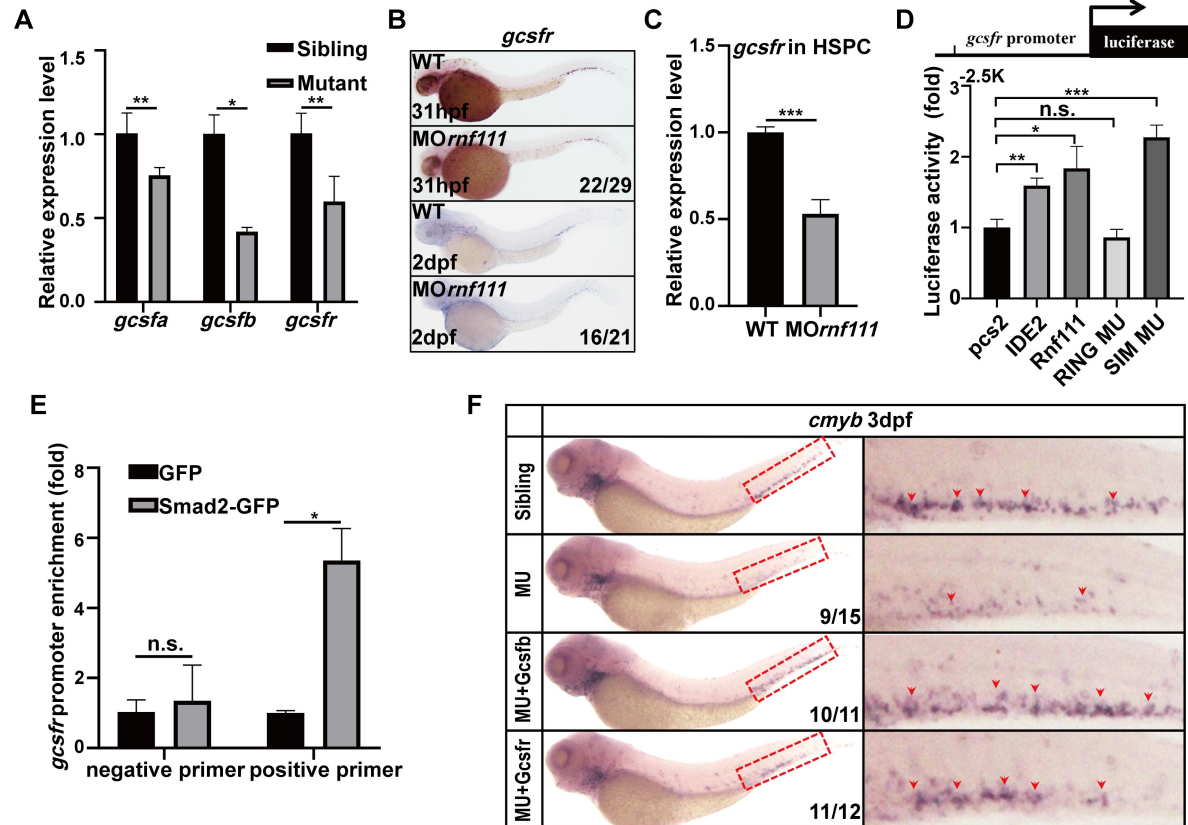
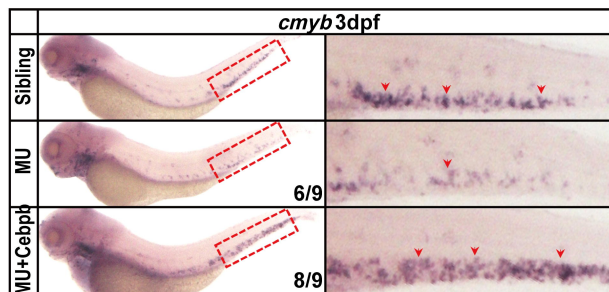
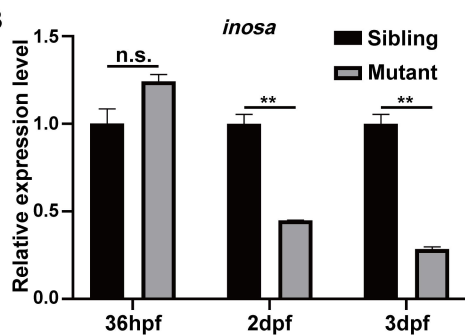
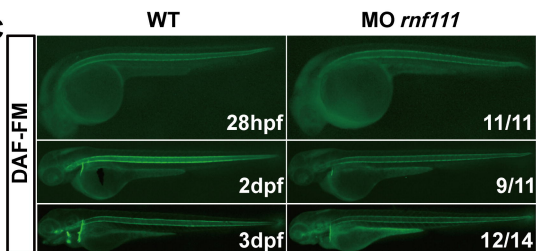
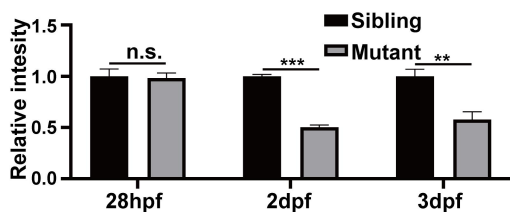
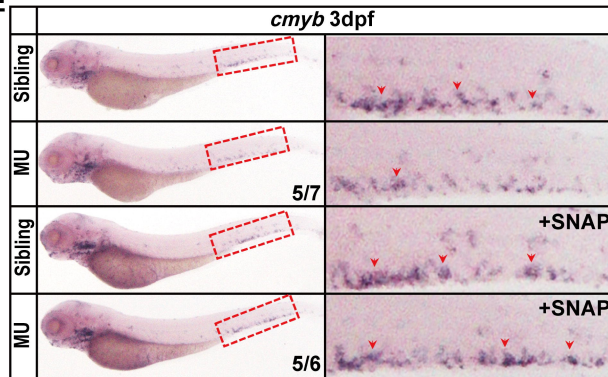
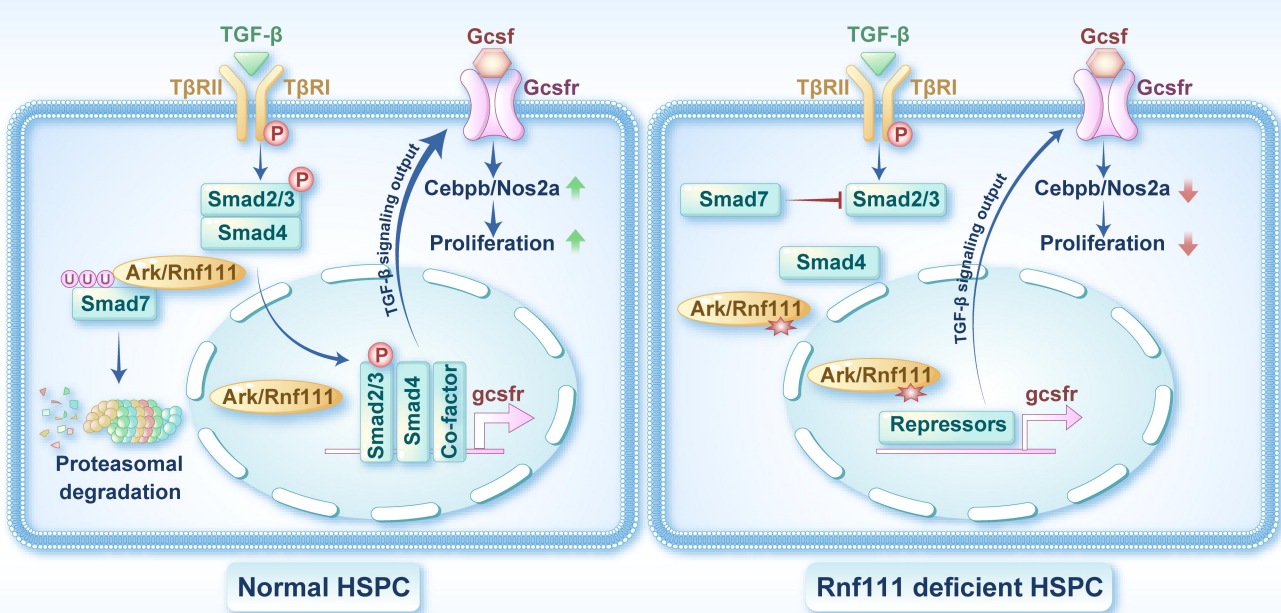


Figure 7**A****B****C****D****E**



Supplementary data

Supplementary methods

Supplementary references

Supplementary figures S1 to 7

Supplementary table S1

Supplementary methods

Zebrafish mutant generation

For generating *Rnf111* knockout zebrafish by CRISPR/Cas9 technology, guide RNA (gRNA) was designed by ZiFiT Targeter software (<http://zifit.partners.org/ZiFiT>). The sequence of target site was as follows: 5'-GGCGGCTGCTGAGCAGCTAC-3'. Cas9 RNA and gRNA were co-injected into one-cell stage zebrafish embryos to obtain F0 generation. For identifying the genotypes, genomic DNA extracted from adult tail or embryos was amplified and DNA products (262 bp) were digested with AluI. Samples from the mutant strand were not digested into two fragments, while those from wildtype strand were fully cleaved. The PCR primers were as follows: Forward primer: TCCTCTTCCTCCTCCGTAA; Reverse primer: TCTGCTCTCATCTGATTGGAGA.

Whole-mount in situ hybridization (WISH)

Plasmid constructs containing a portion of the coding sequence were firstly linearized by certain restriction endonuclease. Then T3 or T7 polymerase (Ambion, Life Technologies, Carlsbad, CA, USA) were used for synthesizing digoxigenin (DIG)-labeled RNA probes. Whole-mount mRNA in situ hybridization (WISH) was performed according to the procedure described previously.¹ Alkaline phosphatase-coupled anti-digoxigenin Fab fragment antibody (Roche, Basel, Switzerland) was used to recognize the digoxigenin-labeled probes. And then BCIP/NBT staining (Vector Laboratories, Burlingame, CA, USA) was carried out to detect the signaling.

Morpholinos and mRNA microinjection

Zebrafish embryos at the single-cell stage were utilized for morpholinos (MO) and mRNA injection. Morpholino oligonucleotides were designed by and ordered from Gene Tools. The MO sequence of *rnf111* was 5'-GCCGAAATCTCACTTTCATGGCGA-3' and the MO sequence of *gcsfr* was 5'-AAGCACAAGCGAGACGGATGCCAT-3', which is the same as reported previously.² Transcribing linearized plasmids with mMachine SP6 kit (Invitrogen, Thermo Fisher, USA) produced capped mRNA samples, which were subsequently purified and diluted to 100 ng/ul (*rnf111*, *rnf111* RING MU, *rnf111* SIM MU, *gcsfb* and *gcsfr* RNA) or 50 ng/ul (*cebpb* RNA) for injection at one-cell stage of embryos.

Quantitative real-time PCR

Reverse transcription was performed using RevertAid First Strand cDNA Synthesis Kit (Life Technologies) in accordance with the manufacturer's instructions. Gene expression levels were

comparatively assessed using reverse transcription polymerase chain reaction (PCR) (Applied Biosystems, Foster City, CA, USA). Each sample was tested in triplicate and housekeeping gene β -actin was chosen for performing the normalization of gene expression using the $\Delta\Delta C_t$ method.³ The results were analyzed with GraphPad Prism software. The final results were expressed as the mean \pm S.D.

Immunofluorescence assay

Tg (*cmyb*:EGFP)⁴ embryos (3 days post-fertilization, dpf) were fixed in 4% paraformaldehyde (PFA) overnight at 4°C. Following a sequence of dehydration and rehydration steps, the embryos underwent treatment with Proteinase K (10 ug/ml; Sigma-Aldrich) for 30 min at room temperature (RT) and then acetone treatment for 10 minutes at -20°C. Subsequently, the embryos were permeabilized through incubation in a solution containing 0.1% Triton X-100 + 0.1% sodium citrate in PBS for 15 minutes at RT. After blocking for 1 hour at RT with blocking solution (2 mg/ml BSA + 10% FBS + 0.3% Triton-X100 + 1%DMSO in PBST), the embryos were simultaneously stained with mouse anti-green fluorescent protein (GFP) (Invitrogen, Carlsbad, CA, USA) and rabbit anti-p-Smad2 (Ser465/467)/ Smad3 (Ser423/425) (Cell signaling) primary antibodies during an overnight incubation at 4°C. The secondary antibodies used for detection included Alexa Fluor 488-conjugated anti-mouse (Invitrogen) and Alexa Fluor 594-conjugated anti-rabbit (Invitrogen).

Bromodeoxyuridine (BrdU) and enhanced green fluorescent protein (EGFP) double immunostaining.

The 3 dpf transgenic Tg (*runx1*: EGFP)⁵ and Tg (*cmyb*:EGFP) embryos were firstly incubated with 10 mM Bromodeoxyuridine (BrdU) (Sigma) for 30 minutes, followed by a 2-hour incubation in egg water. Subsequently, the embryos were fixed in 4% PFA overnight at 4°C. Then, after dehydrated and rehydrated at RT, the embryos were digested with proteinase K (10 ug/ml; Sigma-Aldrich) at 30°C for 30 min and treated with acetone at -20°C for 30 min. After blocked with blocking solution (PBS + 0.3% Triton X-100 + 1% DMSO + 10 mg/ml bovine serum albumin + 10% normal goat serum) for 2 hours, the embryos were sequentially immunostained by rabbit anti-GFP primary antibody (1:500; Invitrogen) and Alexa Fluor 488-conjugated anti-rabbit secondary antibodies (1:500; Invitrogen). Then, the embryos were treated with 2 N HCl for 1 hour and further stained with mouse anti-BrdU (1:50; Roche) and rabbit anti-GFP antibodies simultaneously. Finally, Alexa Fluor 594-conjugated anti-mouse and Alexa Fluor 488-conjugated anti-rabbit (1:500;

Invitrogen) were used as secondary antibodies.

Cell culture and luciferase reporter assay

HEK293T cells were seeded in 24-well plates and cultured in DMEM (Life technologies, Grand Island, NY, USA) with 10% Fetal Bovine Serum (Life technologies, Grand Island, NY, USA) at 37°C with 5% CO₂ atmosphere. Effectene Transfection Reagent (QIAGEN) was used for plasmid transfections according to the manufacturer's instructions. For the luciferase reporter assay, cells were harvested 36-48 hours following transfection and then detected using the Dual Luciferase Reporter Assay Kit (Promega, Madison, WI, USA).

Immunohistochemistry

The 3 dpf embryos were fixed in 4% PFA overnight at 4°C. After dehydration and rehydration, the embryos were treated with Proteinase K (10 µg/ml; Sigma-Aldrich) for 30 min at RT and then treated with acetone for 10 minutes at -20°C. Then, the embryos were incubated with the rabbit anti-p-Smad2 (Ser465/467)/ Smad3 (Ser423/425) primary antibodies and alkaline phosphatase conjugated anti-rabbit secondary antibodies at 4°C overnight. BCIP/NBT staining was performed to detect the signaling.

Western blot

For Western blot analysis, embryos were deyolked and homogenized in lysis buffer containing protease inhibitor cocktail (Roche) and phosphatase inhibitor PhosSTOP™ (Roche) as previously reported.⁶ Total proteins were separated by 10% SDS-PAGE (Sigma-Aldrich, St. Louis, MO, USA) and transferred onto nitrocellulose membranes (GE Healthcare Life sciences, Pittsburgh, PA, USA). The membrane was blocked by 5% non-fat milk at RT for 1 hour, followed by overnight incubation with primary antibodies at 4 °C overnight. After incubated with secondary antibody at RT for 2 hours, SuperSignal West Pico Chemiluminescent Substrate (Thermo Scientific, Rochford, IL, USA) was used to detect the signal. The antibodies used in western blot analysis were as follows: Rabbit anti-p-Smad2 (Ser250) (Beyotime, Shanghai), Rabbit anti-p-Smad3 (Ser423/425) (Beyotime, Shanghai), rabbit anti-Smad2 antibody (Abmart, Shanghai), rabbit anti-Smad3 antibody (Abmart, Shanghai), mouse anti-Smad7 monoclonal antibody (R&D Systems, USA) and mouse anti-GAPDH Monoclonal antibody (Proteintech Group, USA).

Chromatin immunoprecipitation PCR (ChIP-PCR)

GFP and Smad2-GFP RNA were injected to embryos at one cell stage and harvested at 48 hpf.

Following homogenization and fixation, SimpleChIP® Enzymatic Chromatin IP Kit (Cell Signaling Technology) was used for immunoprecipitating cross-linked chromatin with anti-GFP antibody (Abcam). The immunoprecipitated samples were analyzed by quantitative PCR using primer pairs listed in the supplementary table.

Chemical treatment

Embryos were treated with 10 μ M S nitroso N-acetylpenicillamine (SNAP) (Sigma-Aldrich) at bud stage as previously reported.⁷ Definitive endoderm 2 inducer (IDE2) (Abcam) at the concentration of 1 μ M was used to activate the phosphorylation of Smad2 from 16 hpf to 3 dpf. Nitric oxide synthase 2 (NOS2)-specific inhibitor 1400W (Selleck) was used to treat embryos at a concentration of 1 mM from 1 dpf to 3 dpf.

Supplementary references

1. Thisse C, Thisse B. High-resolution in situ hybridization to whole-mount zebrafish embryos. *Nat Protoc.* 2008;3(1):59-69.
2. Hall CJ, Flores MV, Oehlers SH, et al. Infection-responsive expansion of the hematopoietic stem and progenitor cell compartment in zebrafish is dependent upon inducible nitric oxide. *Cell Stem Cell.* 2012;10(2):198-209.
3. Livak KJ, Schmittgen TD. Analysis of relative gene expression data using real-time quantitative PCR and the $2^{-\Delta\Delta C(T)}$ Method. *Methods.* 2001;25(4):402-408.
4. North TE, Goessling W, Walkley CR, et al. Prostaglandin E2 regulates vertebrate haematopoietic stem cell homeostasis. *Nature.* 2007;447(7147):1007-1011.
5. Zhang P, He Q, Chen D, et al. G protein-coupled receptor 183 facilitates endothelial-to-hematopoietic transition via Notch1 inhibition. *Cell Res.* 2015;25(10):1093-1107.
6. Link V, Shevchenko A, Heisenberg CP. Proteomics of early zebrafish embryos. *BMC Dev Biol.* 2006;6(1).
7. Lu X, Li X, He Q, et al. miR-142-3p regulates the formation and differentiation of hematopoietic stem cells in vertebrates. *Cell Res.* 2013;23(12):1356-1368.

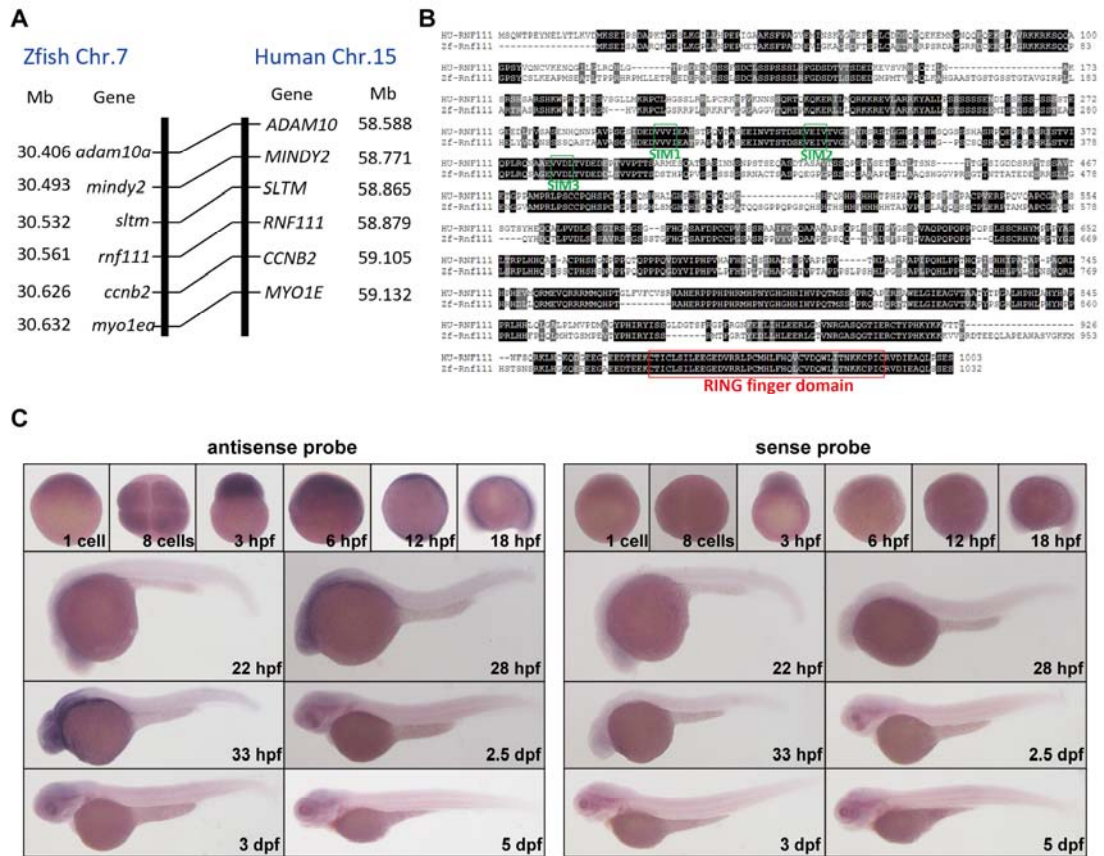


Figure S1.* Conservation analysis of zebrafish *rnf111*. (A) Synteny analysis of human *RNF111* and zebrafish *rnf111* loci. (B) The alignment of multiple sequences indicates the evolutionary conservation of human RNF111 and zebrafish Rnf111 proteins. The sequence in the green box represents the SUMO-interacting motifs (SIM). The sequence in the red box represents the RING finger domain. (C) WISH result showed that *rnf111* is a maternal gene, expressing ubiquitously including hematopoietic tissues. SIM: SUMO-interacting motifs; hpf: hours post-fertilization; dpf: days post-fertilization; WISH: whole-mount in situ hybridization.

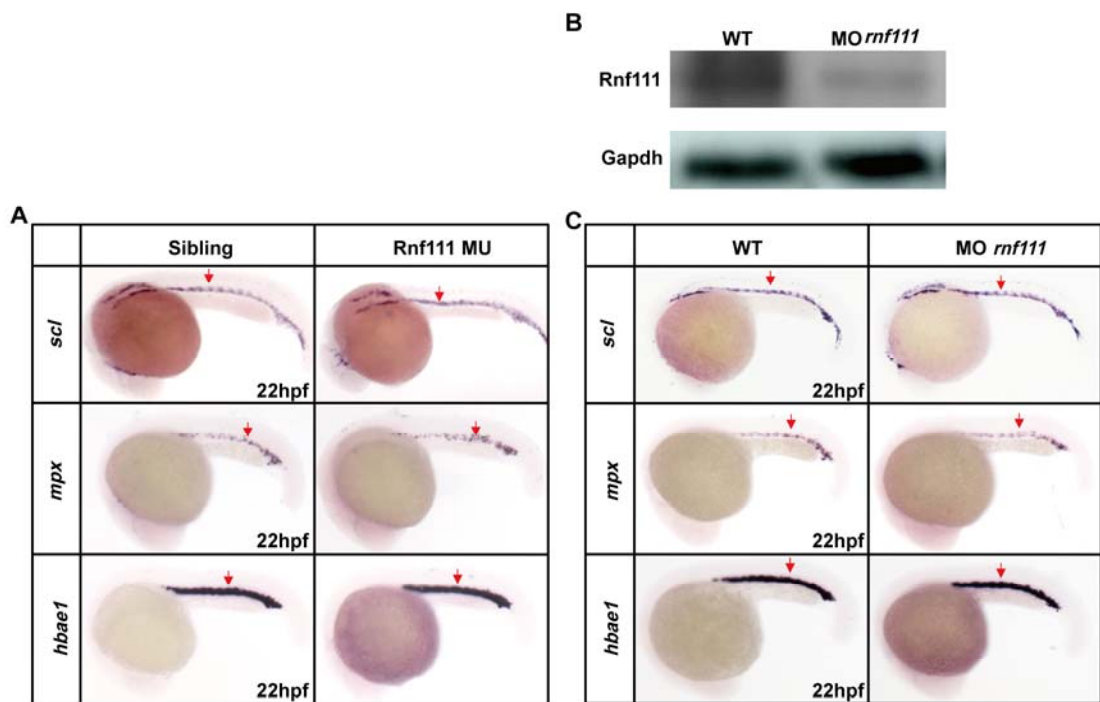


Figure S2.* The phenotypes of primitive hematopoiesis in Rnf111 deficient embryos. (A) WISH analysis of *scl*, *mpx* and *hbae1* at 22 hpf in Rnf111 mutants. (B) Western blot of Rnf111 indicated the protein level of Rnf111 was sharply decreased at 2 dpf in *rnf111* morphants. (C) WISH analysis of *scl*, *mpx* and *hbae1* at 22 hpf in *rnf111* morphants. All experiments were independently replicated at least three times. MU: Rnf111 mutants with deletion of 4bp nucleotides; hpf: hours post-fertilization; WT: wildtype; MO *rnf111*: *rnf111* morphants; WISH: whole-mount in situ hybridization; dpf: days post-fertilization.

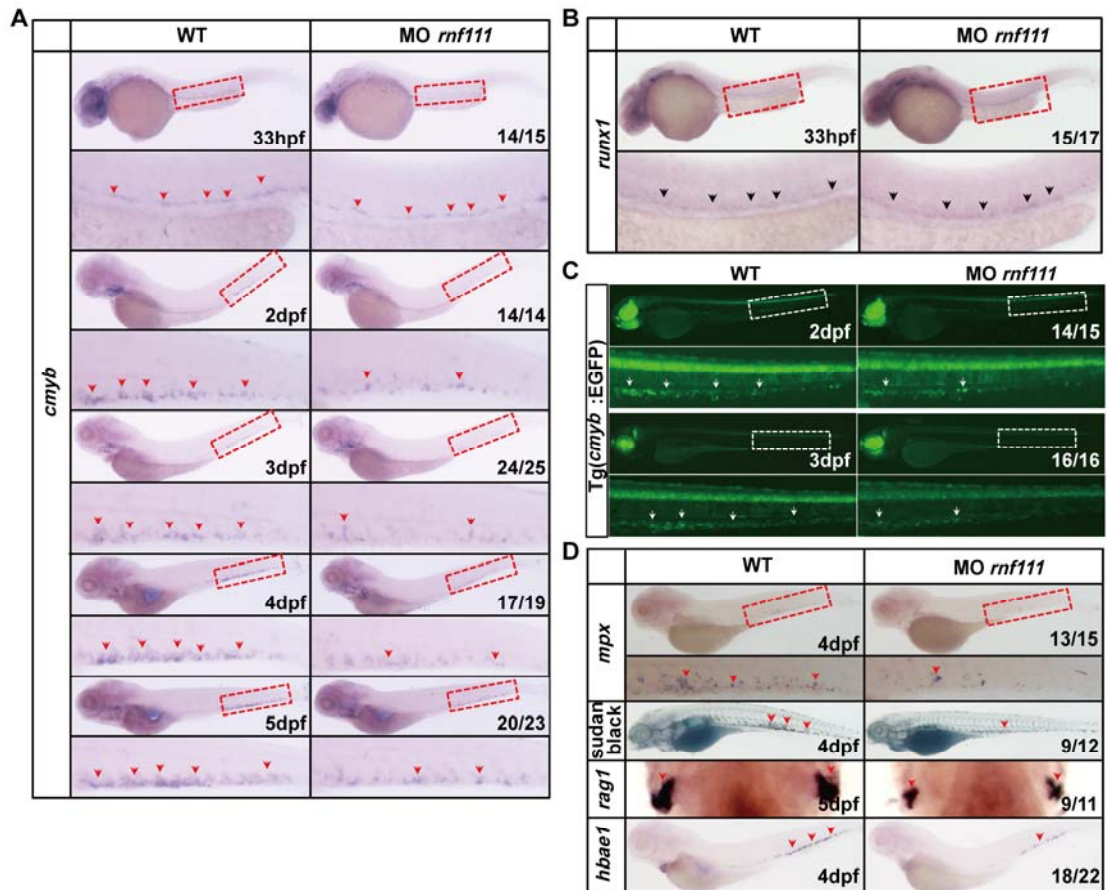


Figure S3.* Impairment of definitive hematopoiesis in *rnf111* morphants. (A) WISH analysis of *cmyb* expression from 33 hpf to 5 dpf. In *rnf111* morphants, *cmyb* expression was normal at 33 hpf and decreased from 2 dpf until all subsequent stages of development. Red arrows indicate *cmyb*-positive HSPC in the AGM or CHT. (B) WISH analysis of *runx1* expression at 33 hpf. Black arrows indicate *runx1*-positive HSPC in the AGM. (C) Fluorescent images of Tg(*cmyb*:EGFP) embryos. White arrows indicate GFP-positive HSPC in the CHT. (D) WISH analysis of key hematopoietic markers and Sudan Black B staining in *rnf111* morphants and wildtype embryos. Expressions of myeloid-specific marker *mpx*, lymphocyte maker *rag1*, mature erythrocyte marker *hbae1* and Sudan Black signal were decreased in *rnf111* morphants. All experiments were independently replicated at least three times. WT: wildtype; MO *rnf111*: *rnf111* morphants; hpf: hours post-fertilization; dpf: days post-fertilization; Tg: transgenic; EGFP: enhanced green fluorescent protein; WISH: whole-mount in situ hybridization; GFP: green fluorescent protein; HSPC: hematopoietic stem and progenitor cell; CHT: caudal hematopoietic tissue; AGM: aorta–gonad–mesonephros.

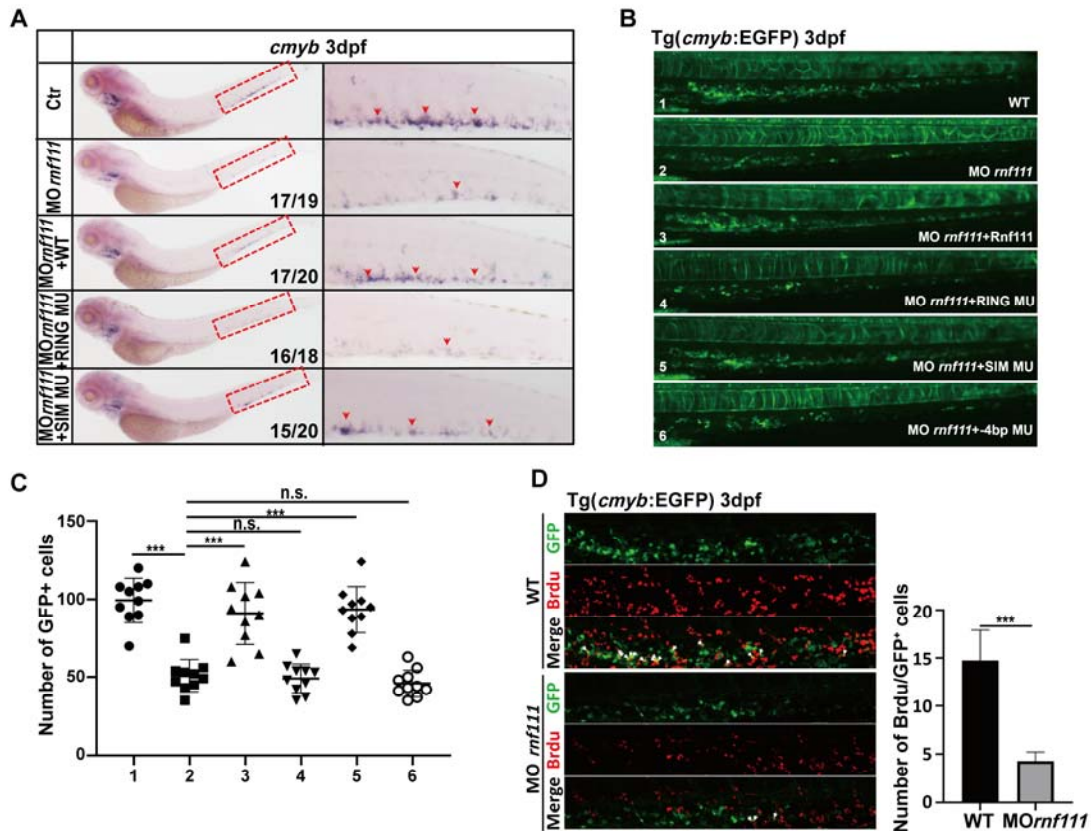


Figure S4.* Analysis of rescue efficiency of different Rnf111 mRNAs in *rnf111* morphants and Brdu assay in Tg(*cmyb*:EGFP) embryos at 3 dpf. (A) WISH analysis of rescue efficiency of Rnf111 WT, Rnf111 RING mutant and Rnf111 SIM mutant RNA. Red arrows indicate *cmyb*-positive HSPC. (B) Fluorescent images of rescue efficiency of Rnf111 RNAs on HSPC in *rnf111* morphants. (C) Statistical analysis of *cmyb*-GFP⁺ cell numbers in corresponding groups listed in Figure S4B. The data are presented as mean \pm S.D. with *** $P < 0.001$ and n.s.: no significant difference. (D) Double immunostaining of *cmyb*-EGFP and anti-Brdu in the CHT region of Tg(*cmyb*-EGFP) line at 3 dpf. White arrows indicate Brdu and *cmyb*-EGFP double positive cells. All experiments were independently replicated at least three times. dpf: days post-fertilization; Ctr: control; MO *rnf111*: *rnf111* morphants; WT: wildtype; RING MU: Rnf111 RING mutant with the RING domain mutated; SIM MU: Rnf111 SIM mutant with three SUMO-interacting motifs all mutated; SIM: SUMO-interacting motif; HSPC: hematopoietic stem and progenitor cell; GFP: green fluorescent protein; Brdu: Bromodeoxyuridine; CHT: caudal hematopoietic tissue.

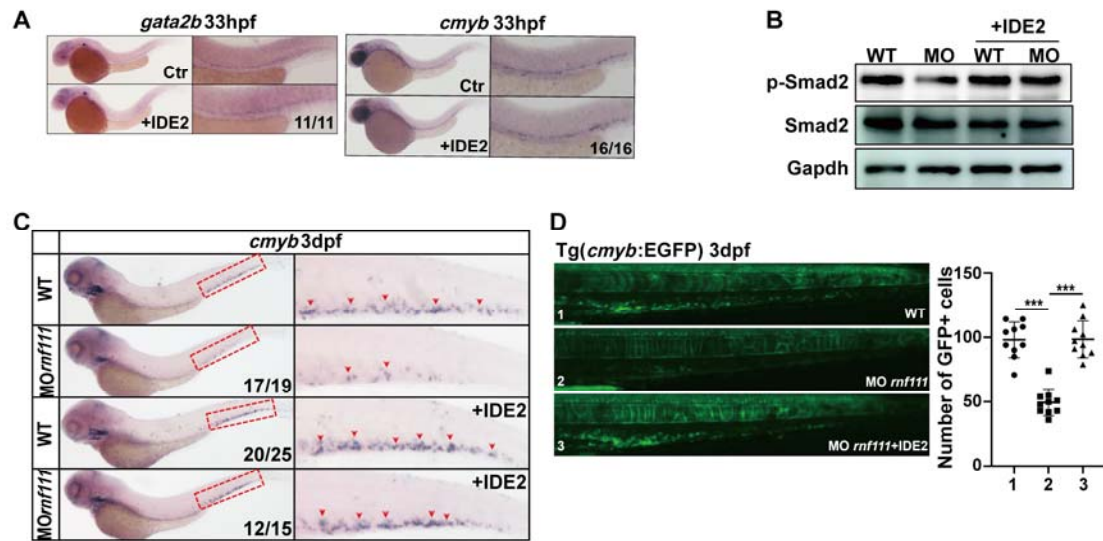


Figure S5.* Rescue efficiency of IDE2 in *rnf111* morphants. (A) WISH assay of HE marker *gata2b* and HSPC marker *cmyb* in IDE2 treated WT embryos from 10 hpf to 33 hpf. (B) Western blot analysis of phosphorylation of Smad2 with or without IDE2 treatment in *rnf111* morphants. (C) WISH analysis of rescue efficiency of IDE2 in *rnf111* morphants. Red arrows indicate *cmyb*-positive HSPC in the CHT. (D) Fluorescent images of rescue efficiency of IDE2 on HSPC in *rnf111* morphants and statistical analysis of *cmyb*-GFP⁺ cell number in different groups. The data are presented as mean \pm S.D. with ***P < 0.001. All experiments were independently replicated at least three times. hpf: hours post-fertilization; Ctr: control; IDE2: definitive endoderm 2 inducer; WT: wildtype; MO *rnf111*: *rnf111* morphants; WISH: whole-mount in situ hybridization; HE: hemogenic endothelium; HSPC: hematopoietic stem and progenitor cell; CHT: caudal hematopoietic tissue.

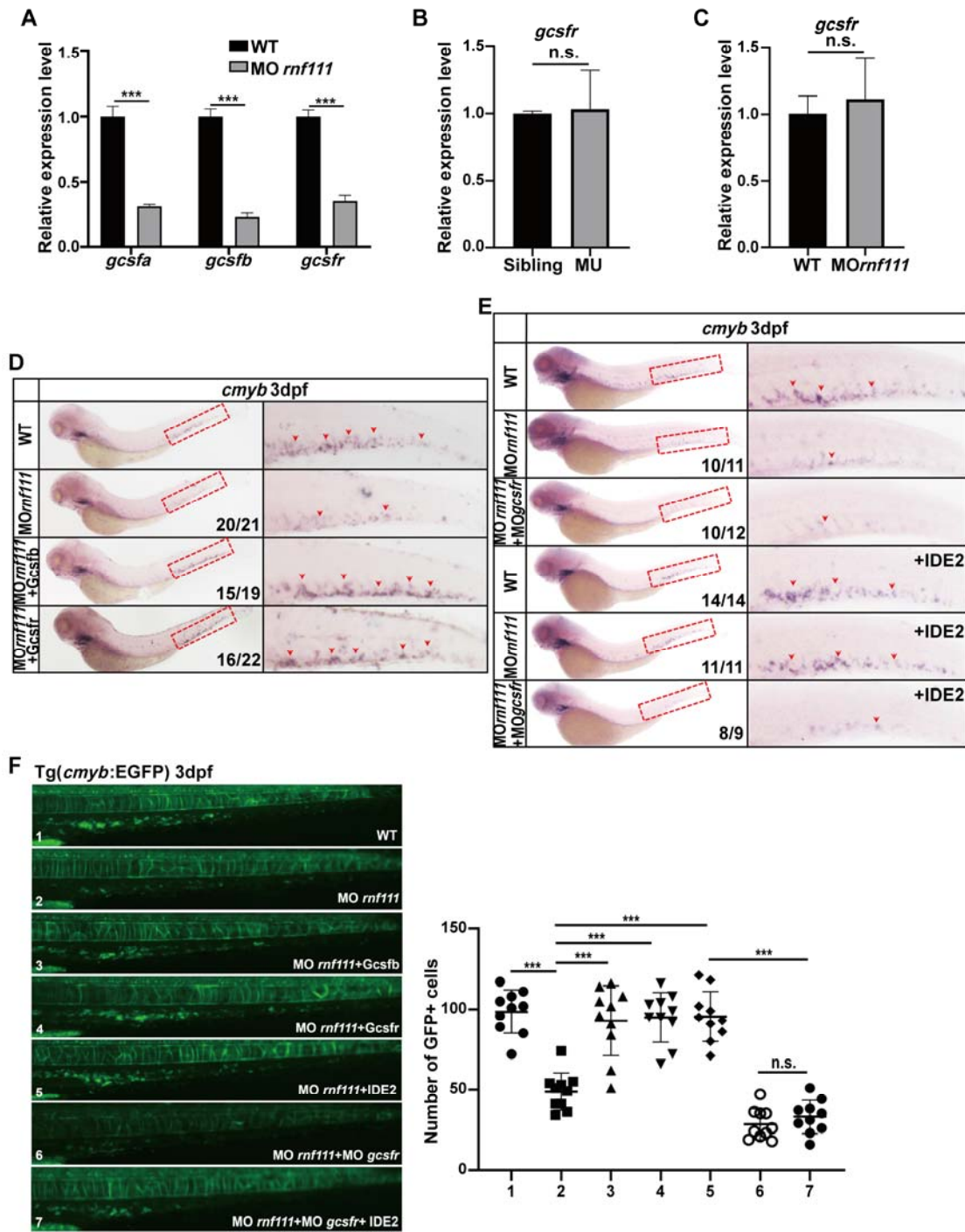


Figure S6.* Analysis of the function of Gcsfr involved in Rnf111 regulating HSPC development.

(A) RT-qPCR of *gcsfa*, *gcsfb* and *gcsfr* at 3 dpf. (B) RT-qPCR of *gcsfr* in siblings and mutants at 36 hpf. (C) RT-qPCR of *gcsfr* in AGM region of WT and *rnf111* morphants at 31 hpf. (D) Rescue assay of *gcsfb* and *gcsfr* RNA in *rnf111* morphants. (E) Compared with *rnf111* MO + IDE2 group, *gcsfr* MO blocked the rescue effect of IDE2 on HSPC in *rnf111* morphants. (F) Fluorescent images of rescue efficiency of different treatment on HSPC in *rnf111* morphants and statistical analysis of

cmyb-GFP⁺ cell number in different groups. The data are presented as mean ± S.D. with ***P < 0.001 and n.s.: no significant difference. All experiments were independently replicated at least three times. Red arrows indicate *cmyb*-positive HSPC in the CHT. WT: wildtype; MO *rnf111*: *rnf111* morphants; dpf: days post-fertilization; MO: morpholino; IDE2: definitive endoderm 2 inducer; WISH: whole-mount in situ hybridization; RT-qPCR: real-time quantitative polymerase chain reaction; HSPC: hematopoietic stem and progenitor cell; CHT: caudal hematopoietic tissue.

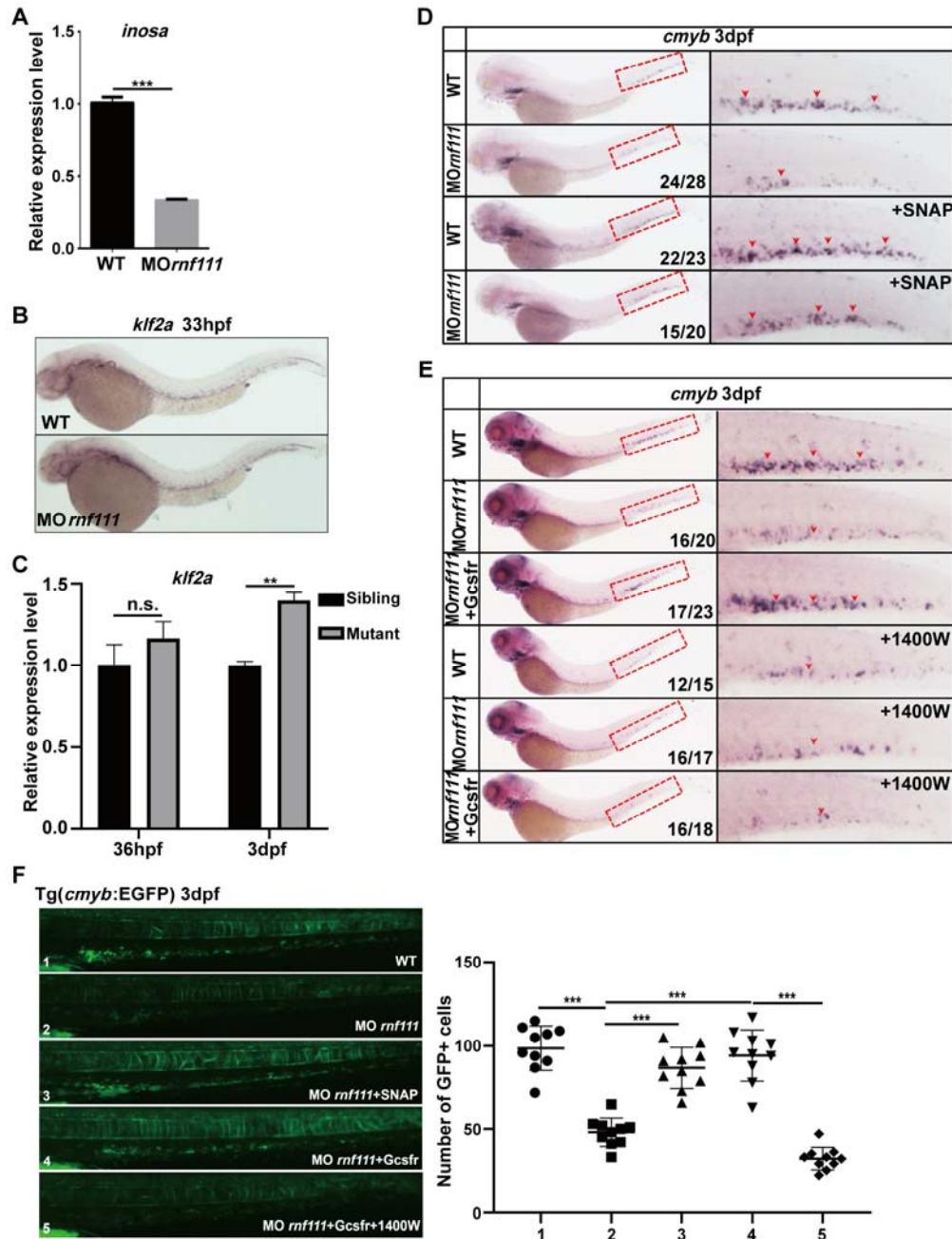


Figure S7.* Analysis of the function of NO signal involved in Rnf111 regulating HSPC development. (A) RT-qPCR result of *inosa* in *rnf111* morphants compared with WT embryos at 3 dpf. (B) WISH assay of *klf2a*. (C) RT-qPCR result of *klf2a* in siblings and mutants. (D) Rescue effect of NO agonist SNAP on *cmyb* expression was observed in *rnf111* morphants. (E) In the absence of 1400W, *gcsfr* RNA can rescue the HSPC defect in *rnf111* morphants. (F) Fluorescent images of rescue efficiency of different treatment on HSPC in *rnf111* morphants and statistical analysis of *cmyb*-GFP⁺ cell number in different groups. The data are presented as mean ± S.D. with **P < 0.01, ***P < 0.001 and n.s.: no significant difference. All experiments were independently

replicated at least three times. In contrast, the rescue effect of *gcsfr* RNA disappeared after 1400W treatment. WT: wildtype; MO *rnf111*: *rnf111* morphants; hpf: hours post-fertilization; dpf: days post-fertilization; SNAP: S nitroso N-acetylpenicillamine; 1400W: a NOS2-specific inhibitor; WISH: whole-mount in situ hybridization; RT-qPCR: real-time quantitative polymerase chain reaction; HSPC: hematopoietic stem and progenitor cell.

qPCR primers	zf-gcsfa-F	AACTACATCTGAACCTCCTG
	zf-gcsfa-R	GACTGCTCTTCTGATGTCTG
	zf-gcsfb-F	GGAGCTCTGCGCACCCAACA
	zf-gcsfb-R	GGCAGGGCTCCAGCAGCTTC
	zf-gcsfr-F	CGACTACAGACTCACTACAG
	zf-gcsfr-R	AGTATCAGCGTGGATGTTC
	zf-nos2a-F	CATCTCCCAGAAGACCCCAG
	zf-nos2a-R	GGGGCTAATTGCTGACCTG
	zf-klf2a-F	ACCTTAACTGGGACGACTGG
	zf-klf2a-R	ATCCTTCCACCTGTTCTCCC
	zf- β -actin-F	GCTGTTTTCCCCTCCATTGTT
	zf- β -actin-R	TCCCATGCCAACCATCACT
	negative primer-F	CGCCAGACAGTGACAAAAGA
	negative primer-R	ATCAGCGGCTCACATAAAGG
	positive primer-F	TTCGGTTTGTGCTTGTGGTT
positive primer-R	TTGTGTAGTTTGTGCCCAGC	

Table S1. The sequence of primers used in quantitative polymerase chain reaction. qPCR: quantitative polymerase chain reaction; zf: zebrafish; F: forward primer; R: reverse primer.